Lagrange/Vandermonde MUI Eliminating User Codes for Quasi-Synchronous CDMA in Unknown Multipath

Anna Scaglione, *Member, IEEE*, Georgios B. Giannakis, *Fellow, IEEE*, and Sergio Barbarossa, *Member, IEEE*

***Abstract*—A family of codes for low-complexity quasi-synchronous code division multiple access (CDMA) systems is developed in order to eliminate multiuser interference (MUI) completely in the presence of unknown and even rapidly varying multipath. Judiciously designed precomputable symbol-periodic user codes, which we term Lagrange or Vandermonde, and the corresponding linear receivers offer a generalization of orthogonal frequency division multiplexing (OFDM), which are especially valuable when deep-fading, carrier frequency errors, and Doppler effects are present. The flexibility inherent to the designed transceivers is exploited to derive transmission strategies that cope with major impairments of wireless CDMA channels. The symbol-periodic code design is also generalized to include the class of aperiodic spreading and orthogonal multirate codes for variable bit rate users. Performance analysis and simulations results illustrate the advantages of the proposed scheme over competing alternatives.**

***Index Terms*—Channel equalization, code division multiple access, multiuser and multicarrier communications.**

I. Introduction

THE recognition of code division multiple access (CDMA) as a promising multiple access scheme has rendered it a viable choice for the next generation cellular standard (UMTS/IMT-2000) [15]. Denoting by T the symbol duration and by B the available bandwidth, the maximum possible number of orthogonal codes is approximately equal to the time-bandwidth product TB [2]. CDMA systems use a large TB to accommodate a large number of users M, with $BT \approx BT_cM$, where T_c denotes the chip duration [24]. Although CDMA systems can provide higher capacity than TDMA systems in cellular networks, their performance depends on the number of active users and their rates. Higher aggregate data rates cause performance degradation when multiuser interference (MUI) increases. As a result, only underloaded CDMA systems outperform TDMA and FDMA if simple matched filter receivers are employed. However, it is possible to achieve full capacity while preserving low error probability when more complex receivers are deployed, based on the active users' codes and channel status information. Those include joint multiuser detectors and successive decoding schemes [24].

Zero-forcing (ZF) or minimum mean-square error (MMSE) linear multiuser detectors outperform matched filter receivers because (under certain constraints) they are capable of handling asynchronous users, near-far effects, and multipath (see, e.g., [9], [13]). Linear solutions are valuable because they simplify multiuser detection, but deriving the corresponding equalizers often involves complex operations. An exception is given by the receiver design in [7], but the price paid is that to achieve MUI elimination, the system should face a consistent reduction in the maximum possible aggregate rate. Moreover, since, in wireless communications, multipath channels are unknown, training sequences are periodically transmitted to estimate the active users' channel parameters. Following [21], blind approaches based on subspace methods or adaptive inverse filtering have been proposed recently in order to obviate bandwidth-consuming training sequences [3], [11], [14], [20], [25]. They rely only on the received data and on the knowledge of the codes, but they have relatively high complexity when subspace channel estimation is employed or reduced capability to suppress MUI, especially when simple (e.g., LMS-type) receivers are adopted to equalize fast varying channels.

Novel low-complexity CDMA transceivers are introduced in [17] that are capable of eliminating MUI deterministically in the presence of *unknown* and even rapidly varying multipath, provided that the channel has finite memory and that the users' asynchronism is limited. More important, the resulting receivers in [17] do not rely on the received data because they are precomputable from appropriately designed user codes. Compared with competing solutions such as [19], we will show herein that our design also leads to a class of codes capable of perfect MUI elimination with minimum TB product. Unlike blind CDMA systems that mitigate MUI at the receiver, the proposed system selects user codes so that MUI is suppressed, *irrespective* of FIR frequency selective multipath, which is converted into a flat fading one. The latter is analogous to the property exhibited by orthogonal frequency-division multiple access (OFDMA), which will turn out to be a special case of our general code design algorithm. We focus, as with OFDMA, on a quasisynchronous (QS) system, where users' asynchronism is limited

Manuscript received January 11, 1999; revised February 18, 2000. This work was supported by NSF CCR under Grant 98-05350 and the Wireless Initiative Grant 99-79443. The associate editor coordinating the review of this paper and approving it for publication was Prof. Dimitrios Hatzinakos.

A. Scaglione and G. B. Giannakis are with the Department of Electrical and Computer Engineering, University of Minnesota, Minneapolis, MN 55455 USA.

S. Barbarossa is with the Information and Commmunication (INFOCOM) Department, University of Rome "La Sapienza," Roma, Italy.

Publisher Item Identifier S 1053-587X(00)04944-8.

to only a few chips.[1] Under the QS model, our transmission strategy weds FDMA's advantage of enabling channel independent MUI-free reception with TDMA's improved performance that are made by design independent of the number of active users. In addition, our proposed system preserves the attractive features of CDMA in terms of efficiency and provision for MMSE and RAKE receivers that for a known channel and negligible MUI are robust against common impairments affecting wireless channels.

In Section II, the discrete time model is described. Our Lagrange-Vandermonde (LV) code design is developed in Section III, where we also establish the *uniqueness* of the LV transceivers. In Section IV, we derive the dual solution, namely, the Vandermonde-Lagrange (VL) transceivers, which offer increased flexibility in the code management. The current trend within the UMTS standardization process in Europe foresees adoption of the so-called orthogonal variable spreading factor (OVSF) codes to accommodate variable bit rate users. However, OVSF codes are highly sensitive to multipath because their cross-correlations are not negligible. Building on the LV scheme, we provide in Section V a class of codes that enables multirate services and guarantees MUI elimination at the expense of a small reduction in the information rate due to the insertion of guard times. In the same section, we also derive the class of MUI-free long codes, namely, those codes with duration greater than the symbol period (the long codes currently adopted by IS-95, for example). In Section VI, we study the performance, which is expressed in terms of error and outage probabilities, for frequency-selective Rayleigh fading channels. We also provide theoretical performance analysis of our system in the presence of multipath and Doppler shifts. In Section VII, we compare the so-called root control with power control strategies as antifading techniques. We also introduce redundant coding against channel fading and root hopping to balance quality of service provided to different users.

II. Modeling and Motivation

The block diagram in Fig. 1 represents the uplink of a CDMA system, which is described in terms of its equivalent discrete-time baseband model, where signals, codes, and channels are represented by samples of their complex envelopes taken at the chip rate (see also [20] and [23]). The continuous time signal $u_{m,c}(t)$ transmitted by the mth user is a PAM waveform $u_{m,c}(t) = \Sigma_{n=-\infty}^{\infty} u_m(n)\phi(t - nT_c)$, where

$u_m(n)$ mth user's encoded data;
T_c chip period;
$\phi(t)$ pulse-shaping filter.

Upsamplers and downsamplers serve the purpose of multiplexing and demultiplexing (spreading and despreading) by a factor P.

Each of the M users spreads the information sequence $s_m(n)$ with the upsampler and encodes it using the code $c_m(n)$ of length N_c: $u_m(n) = \Sigma_{i=-\infty}^{\infty} s_m(i)c_m(n - iP)$. Denoting by $c_{m,c}(t) := \Sigma_{n=0}^{N_c-1} c_m(n)\phi(t - nT_c)$ the continuous time code and by $T = PT_c$ the symbol duration, the usual representation of the CDMA waveform can be easily obtained as

$$u_{m,c}(t) = \sum_{n=-\infty}^{\infty} \sum_{i=-\infty}^{\infty} s_m(i)c_m(n - iP)\phi(t - nT_c) = \sum_{i=-\infty}^{\infty} s_m(i)c_{m,c}(t - iT). \quad (1)$$

The mth user's transmitted signal $u_{m,c}(t)$ is convolved with the channel impulse response $h_{m,c}(t)$ and filtered at the receiver that is matched to $\phi(t)$. The spectrum $|\Phi(f)|^2$ is assumed to have Nyquist characteristics such that $|\Phi(f)|^2 = 0$ for $|f| > B/2$ with $B \geq 1/T_c$. The bandwidth B is also the user bandwidth for the power spectrum of the user baseband equivalent signal in (1) is (see, e.g., [2])

$$\mathcal{F}\{R_{u_{m,c}}(\tau)\} = \frac{1}{PT_c} S_{s_m}(e^{j2\pi f T_c P})|C_m(e^{j2\pi f T_c})|^2|\Phi(f)|^2 \quad (2)$$

where $\mathcal{F}\{\ \}$ indicates the continuous-time Fourier transform (CFT), $S_{s_m}(e^{j\omega})$ is the discrete Fourier transform (DFT) of the symbol's correlation, $C_m(e^{j\omega})$ is the DFT of the code $c_m(n)$, and $R_{u_{m,c}}(\tau) := E\{u_{m,c}(t)u_{m,c}(t + \tau)\}$. Hence, $|\Phi(f)|^2$ in (2) dictates the signal bandwidth, whereas $C_m(e^{j\omega})$ determines how "spread" in frequency the users' information (for example, if $c_m(n)$ is a PN sequence, $C_m(e^{j\omega})$ is nearly flat) is.

Let us denote the convolution of transmit with receive filters by $R_{\phi\phi}(t)$ and the equivalent discrete time channel impulse response by $h_m(l) := \int_{-\infty}^{\infty} h_{m,c}(\tau)R_{\phi\phi}(lT_c - \tau)\, d\tau$. The mth user's signal component at the chip rate can then be written as

$$x_m(n) = \sum_{i=-\infty}^{\infty} s_m(i) \sum_{l=-\infty}^{\infty} h_m(l)c_m(n - l - iP). \quad (3)$$

In addition to transmit-receive filters and *unknown* multipath effects, the Lth-order FIR[2] filter includes the mth user's asyn-

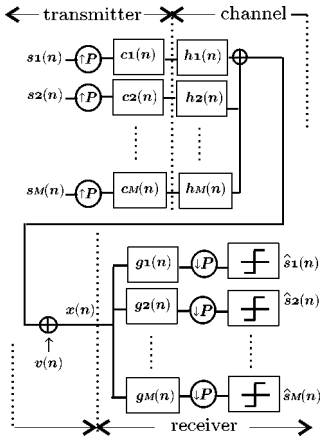

Fig. 1. Multirate discrete-time CDMA model.

[1]In QS-CDMA systems, users attempt to transmit following the base station's clock waveform [18] (or a GPS, as suggested in [5]). However, the received waveforms at the base station are still asynchronous by a few chips due to oscillator drifts and Doppler arising from relative motion between the mobiles and the base station.

[2]The assumption of finite channel support is not exact if the bandwidth is strictly limited, but this approximation is common in wireless environments, where the impulse response support is nearly equal to the maximum path delay plus a few chips.

chronism in the form of delay factors (note that if user 1 is taken as reference, then in the absence of multipath, asynchronism of user m relative to user 1 by d_m chips corresponds to a pure delay channel with $h_m(l) = \alpha_m R_{\phi\phi}((l-d_m)T_c) = \alpha_m \delta(l-d_m)$). The downlink scenario is subsumed in our model because it corresponds to $h_m(l) := h(l), \forall m \in [1, M]$.

The multiplexed data are received in AGN $v_c(t)$ ($v(n) := v_c(nT_c)$), filtered, and sampled at the chip rate to obtain

$$x(n) = \sum_{m=1}^{M} \sum_{i} s_m(i) \sum_{l} h_m(l) c_m(n-l-iP) + v(n). \tag{4}$$

Subsequent processing by the receive filter amounts to correlating $x(n)$ with the sequence $g_m(k)$ of length N_g [or equivalently convolving $x(n)$ with the conjugated and time-reversed $g_m^*(N_g-k)$]. The resulting output is downsampled by P (the combination of filtering and downsampling corresponds to despreading), and the decision is taken over the estimate

$$\hat{s}_m(n) = \sum_{k=0}^{N_g-1} g_m(k) x(nP+k). \tag{5}$$

To cast (4) and (5) in vector-matrix form, let us define the $P \times 1$ vectors

$$\boldsymbol{x}(n) := (x(nP), x(1+nP), \cdots, x(P-1+nP))^T \tag{6}$$

$$\boldsymbol{v}(n) := (v(nP), v(1+nP), \cdots, v(P-1+nP))^T \tag{7}$$

the $(L+1) \times 1$ channel vector

$$\boldsymbol{h}_m := (h_m(0), h_m(1), \cdots, h_m(L))^T \tag{8}$$

and the $P \times (L+1)$ Toeplitz code matrices $\{C_m(q)\}_{m=1}^{M}$ with

$$\{\boldsymbol{C}_m(q)\}_{k,l} := c_m(qP+k-l) \quad k \in 0, \cdots, P-1 \quad l = 9, \cdots, L. \tag{9}$$

Using definitions (6)–(9), we express the kth element of $x(n)$ in (4) as

$$\begin{aligned} \{\boldsymbol{x}(n)\}_k &:= x(k+nP) \\ &= \sum_{m=1}^{M} \sum_{i} s_m(i) \sum_{l=0}^{L} h_m(l) c_m(k-l+(n-i)P) \\ &\quad + v(k+nP) \\ &= \sum_{m=1}^{M} \sum_{i} s_m(i) \sum_{l=0}^{L} \{\boldsymbol{C}_m(n-i)\}_{k,l} h_m(l) \\ &\quad + \{\boldsymbol{v}(n)\}_k. \end{aligned} \tag{10}$$

Observing that $\{\boldsymbol{C}_m(n-i)\boldsymbol{h}_m\}_k = \sum_{l=0}^{L} \{\boldsymbol{C}_m(n-i)\}_{k,l} h_m(l)$, we obtain

$$\boldsymbol{x}(n) = \sum_{m=1}^{M} \sum_{i} s_m(i) \boldsymbol{C}_m(n-i) \boldsymbol{h}_m + \boldsymbol{v}(n). \tag{11}$$

Note that (11) holds even if the code length N_c is greater than P, which is the symbol period in terms of chips, and the resulting system operates as a "partial response" system. This adds flexibility to the system design that will be discussed in Section V. Because the codes convolved with the FIR channel yield a sequence of length N_c+L, we have from (9) that $\boldsymbol{C}_m(q) \equiv \boldsymbol{0}$ for $q < 0$ and $q > \lfloor (N_c+L)/P \rfloor$. Therefore, the summation over i in (11) has only $Q_c := \lceil (N_c+L)/P \rceil$ nonzero terms, and we can rewrite it as

$$\boldsymbol{x}(n) = \sum_{m=1}^{M} \sum_{q=0}^{Q_c-1} \boldsymbol{C}_m(q) \boldsymbol{h}_m s_m(n-q) + \boldsymbol{v}(n) \tag{12}$$

and, for example, if $N_c = P$ and $0 < L < P$, then $Q_c = 2$. Recall now from (5) that $g_m(n)$ has length N_g, define $Q_g := \lceil N_g/P \rceil$, and rewrite (5) as

$$\begin{aligned} \hat{s}_m(n) &= \sum_{k=0}^{Q_g-1} \sum_{p=0}^{P-1} g_m(kP+p) x(nP+kP+p) \\ &= \sum_{k=0}^{Q_g-1} \boldsymbol{g}_m^T(k) \boldsymbol{x}(n+k) \end{aligned} \tag{13}$$

where $\boldsymbol{g}_m(n) := (g_m(nP), g_m(1+nP), \cdots, g_m(P-1+nP))^T$.

Based on (12) and (13), the μth user's symbol estimate is given by (14), shown at the bottom of the page.

Before raising the MUI elimination problem, we wish to underline that our signal model in (1) is symbol periodic. Since our goal is to design the set of user codes that guarantees deterministic channel-irrespective MUI elimination with a linear receive filter and operating in a symbol-by-symbol fashion, a nonsymbol-periodic scheme would not modify the problem in essence.

If MUI in (14) is modeled as additive (approximately) Gaussian noise and one optimizes SNR at the decision point, the simple yet robust matched filter (MF) receiver is obtained as $\boldsymbol{g}_\mu^T(k) \equiv \boldsymbol{h}_\mu^{\mathcal{H}} \boldsymbol{C}_\mu^{\mathcal{H}}(k)$ and is equivalent to the RAKE receiver if all channel paths are combined coherently. However, this solution does not take advantage of the known interfering users' codes. Code design within the MF/RAKE receiver framework consists of selecting codes with good cross correlation properties, which satisfy

$$\boldsymbol{C}_\mu^{\mathcal{H}}(k) \boldsymbol{C}_m(q) \approx \delta(\mu - m) \delta(k-q) \boldsymbol{R}_{cc}(\mu, k) \tag{15}$$

$$\hat{s}_\mu(n) = \sum_{k=0}^{Q_g-1} \sum_{q=0}^{Q_c-1} \boldsymbol{g}_\mu^T(k) \boldsymbol{C}_\mu(q) \boldsymbol{h}_\mu s_\mu(n+k-q) + \underbrace{\sum_{m=1, m\neq\mu}^{M} \sum_{q=0}^{Q_c-1} \sum_{k=0}^{Q_g-1} \boldsymbol{g}_\mu^T(k) \boldsymbol{C}_m(q) \boldsymbol{h}_m s_m(n+k-q)}_{MUI} + \sum_{k=0}^{Q_g-1} \boldsymbol{g}_\mu^T(k) \boldsymbol{v}(n+k). \tag{14}$$

where $\boldsymbol{R}_{cc}(\mu,k)$ is an $(L+1)\times(L+1)$ matrix, and $\delta(k)$ is the Kronecker delta. The term $\delta(\mu-m)$ cancels MUI, whereas $\delta(k-q)$ eliminates ISI. The latter is not strictly necessary because ISI can be handled with equalizers following the RAKE receiver.

It is of interest to show why (15) can only be an approximation. If (15) is to hold exactly, linear algebra requires the $L+1$ columns of all Q_c matrices $\boldsymbol{C}_\mu(k)$ to lie in the left null space $\mathcal{N}(\boldsymbol{C}_m(q))$, $\forall\ \mu\neq m, k\neq q$. Hence, to ensure the absence of MUI, the nullity of $\boldsymbol{C}_\mu(k)$ must satisfy $\boldsymbol{\nu}(\boldsymbol{C}_m(q))\geq(M-1)(L+1)Q_c$. Because $\boldsymbol{C}_m(q)$ in (9) is $P\times(L+1)$, this nullity bound is satisfied either when $\boldsymbol{C}_m(q)\equiv\boldsymbol{0}$, which represents the undesired trivial case, or when $P>(M-1)(L+1)(Q_c-1)$. Such a spreading gain P uses bandwidth inefficiently because for M users and $B=1/T_c$, we require $BT=P>(L+1)(M-1)(Q_c-1)$, which implies a bandwidth increase proportional to the channel memory and Q_c. If, besides MUI and ISI elimination we also want to have maximal ratio combining gain, we must impose (15) with $\boldsymbol{R}_{cc}(\mu,k)\approx\boldsymbol{I}$ so that the RAKE receiver would yield maximum gain $\boldsymbol{h}_m^{\mathcal{H}}\boldsymbol{R}_{cc}(m,q)\boldsymbol{h}_m=\boldsymbol{h}_m^{\mathcal{H}}\boldsymbol{h}_m$. However, imposing $\boldsymbol{R}_{cc}(\mu,k)=\boldsymbol{I}$ would require $\boldsymbol{\nu}(\boldsymbol{C}_m(q))\geq(M-1)(L+1)Q_c-1$, which in turn causes further loss in efficiency because it requires longer codes[3]. In the best scenario, we have $N_c=P$ and $L<P$ so that $Q_c=2$. Observe that MUI and ISI elimination requires $P>(L+1)(M-1)$. This was also observed in [7], where a "delay independent" linear decorrelating receiver was designed and is capable of canceling MUI independent of the users' asynchronism. Unfortunately, as much as one chip of misalignment decreases the system capacity in [7] by 50%. In a nutshell, it is impossible to satisfy (15) exactly unless we underutilize bandwidth by setting $P\approx BT\gg M$.

The natural question is whether it is possible to design codes with perfect MUI cancellation using a linear receiver, as in [13], without knowing the users' channels and without resorting to adaptive blind receivers. Such codes would enable one to cope with the near-far problem effectively and would handle addition of new users as gracefully as TDMA and FDMA. With this motivation, instead of (15), we look for linear reduced-complexity receivers that satisfy

$$\boldsymbol{g}_\mu^T(k)\boldsymbol{C}_m(q)=\delta(\mu-m)\delta(k-q)\boldsymbol{\gamma}^T(\mu,k),\quad\forall\mu,m\in[1,M] \tag{16}$$

where $\boldsymbol{\gamma}(\mu,k)$ is an arbitrary $L\times 1$ vector. For (16) to hold $\forall\mu\neq m$, Q_gM-1 vectors $\boldsymbol{g}_\mu(k)$ must lie in the left null space $\mathcal{N}(\boldsymbol{C}_m(q))$, $\forall\mu\neq m, k\neq q$.

Because $\boldsymbol{\nu}(\boldsymbol{C}_m(q))\geq Q_gM-1$ can be satisfied with $P>Q_gM-1$, let us consider the simplest case $Q_g=1$. If $\text{rank}(\boldsymbol{C}_m(q))=1$, then $P>M-1$ is enough to include $M-1$ vectors in $\mathcal{N}(\boldsymbol{C}_m(q))$ and, thus, satisfy (16). However, the Toeplitz structure of $\boldsymbol{C}_m(0)$ implies that $\text{rank}(\boldsymbol{C}_m(0))=\min(P,L+1)$, and then, $\boldsymbol{\nu}(\boldsymbol{C}_m(0))=P-\min(P,L+1)$. Hence, the most efficient solution corresponding to $BT=M$ is possible only if $P>L$ and, in the ideal $(L=0)$ case, where $h_m(l)=\alpha_m\delta(l)$. The latter leads us to the choice of orthogonal user codes and corresponding matched receivers. For $L>0$, the first $L+1$ rows of $\boldsymbol{C}_m(0)$ form an $(L+1)\times(L+1)$ lower triangular matrix that has full rank if $c_m(0)\neq 0$; hence, with Lth-order multipath, in order to have $\boldsymbol{\nu}(\boldsymbol{C}_m(0))\geq M-1$, we need $P>L$ and spreading $P\geq M+L$. In the next section, we will design codes for $Q_g=1$, minimum spreading $P=M+L$, and minimum code length $N_c=M$ that implies $Q_c=1$. Note from (9) that if $P>L$ whenever $N_c>M$, we have $Q_c>1$; this case will be considered in Section IV, and the resulting code-receiver design is the dual of the one presented in the ensuing section.

[3]Note, however, that $\boldsymbol{C}_m(q)$ is not arbitrary, and thus far, we have not capitalized on the special structure of $\boldsymbol{C}_m(q)$ in (9).

III. Lagrange–Vandermonde CDMA Transceivers

Our discussion in Section II motivates the following assumptions.

- a1) $P-M\geq L$ and $M>L$, where L is the maximum expected order of all channels $\{h_m(l)\}_{m=1}^M$.
- a2) We have codes with $L_g\geq L$ trailing zeros (guard chips); if $L_g=P-M$, then $\{c_m(n)=0\}_{n=M}^{P-1}$.
- a3) $h_1(0)\neq 0$, which is guaranteed when the receiver is synchronized to the user of interest only.

The idea of introducing guard chips, which is called black chip augmentation (BCA), was earlier advocated in [8]. The number of guard chips L_g in a2) may be large in the completely asynchronous case (e.g., in IS-95) because $L=L_d+L_s$ consists of the maximum delay in terms of chips within a symbol among all users relative to the user of interest, plus the maximum delay-spread of the multipath.[4] As L (and hence L_g) increases, our system's information rate decreases. In our QS-CDMA system, $L_d<2,3$ chips, and hence, a1) is satisfied with a small $L_g\leq 7$. On the other hand, users close to the BS will not mask the far users, and power control will undertake only the task of accounting for the dynamic range of the received signals.

Under a1)–a3), $Q_c=1$ and $\boldsymbol{C}_m(q)=\boldsymbol{C}_m(0)\delta(q):=\boldsymbol{C}_m\delta(q)$, and a special case of (12) results:

$$\boldsymbol{x}(n)=\sum_{m=1}^{M}\boldsymbol{C}_m\boldsymbol{h}_m s_m(n)+\boldsymbol{v}(n). \tag{17}$$

Note that thanks to the guard chips in a2), successive data blocks do not interfere with each other; thus, convolution of the mth user's code with the channel is represented as multiplication of the mth user's $P\times(L+1)$ Toeplitz matrix $\boldsymbol{C}_m$ by the channel vector $\boldsymbol{h}_m$. According to (9), and under a1)–a3), matrix $\boldsymbol{C}_m(0)$ reduces to a Sylvester matrix

$$\boldsymbol{C}_m(0):=\boldsymbol{C}_m=\begin{pmatrix} c_m(0) & \cdots & 0\\ \vdots & \ddots & \vdots\\ \vdots & \ddots & c_m(0)\\ c_m(M-1) & \ddots & \vdots\\ \vdots & \ddots & \vdots\\ 0 & \cdots & c_m(M-1)\end{pmatrix}. \tag{18}$$

[4]In a wireless cellular system with cell radius R, $L_d\approx RB/c$, where c is the speed of light; L_s depends essentially on the transmission environment such as hilly terrain or urban.

If $\boldsymbol{g}_\mu := \boldsymbol{g}_\mu(0)$ is the weight vector for receiver μ, its output takes the form

$$\boldsymbol{g}_\mu^T \boldsymbol{x}(n) = \boldsymbol{g}_\mu^T \boldsymbol{C}_\mu \boldsymbol{h}_\mu s_\mu(n) + \sum_{m=1, m\neq\mu}^{M} \boldsymbol{g}_\mu^T \boldsymbol{C}_m \boldsymbol{h}_m s_m(n) + \boldsymbol{g}_\mu^T \boldsymbol{v}(n). \quad (19)$$

Our problem is to design codes $\{c_m(n)\}_{n=0}^{M-1}$ or, equivalently, their polynomials $C_m(z) := \Sigma_{n=0}^{M-1} c_m(n) z^{-n}$ and rely only on these codes to obtain $\boldsymbol{g}_\mu$ so that the MUI [described by the sum in (19)] is eliminated deterministically.

To eliminate MUI irrespective of the channels $\{h_m(l)\}_{m=1}^{M}$, receiver $\boldsymbol{g}_\mu$ must satisfy $\boldsymbol{g}_\mu^T \boldsymbol{C}_m = \boldsymbol{0}^T$ for all $m \neq \mu$; hence, $\boldsymbol{g}_\mu$ in (19) must lie in the intersection of null spaces $\bigcap_{m=1, m\neq\mu}^{M} \mathcal{N}(\boldsymbol{C}_m)$. On the other hand, $\boldsymbol{g}_\mu$ should not annihilate user μ, implying that $\boldsymbol{g}_\mu^T \notin \mathcal{N}(\boldsymbol{C}_\mu)$. Following the same rationale for all users, we arrive at the necessary and sufficient conditions for *channel-independent* MUI elimination:

$$\forall\, \mu \in [1, M] \quad \exists\, \boldsymbol{g}_\mu \colon \boldsymbol{g}_\mu^T \in \mathcal{N}(\boldsymbol{C}_m) \quad \forall m \neq \mu \text{ and } \boldsymbol{g}_\mu^T \notin \mathcal{N}(\boldsymbol{C}_\mu). \quad (20)$$

With arbitrary codes $\{c_m(n)\}_{m=1}^{M}$, the existence of vectors $\{\boldsymbol{g}_\mu\}_{\mu=1}^{M}$ satisfying (20) is not guaranteed. For example, the Walsh–Hadamard codes do not satisfy (20) for $M > 2$; thus, perfect MUI suppression is impossible without relying on channel knowledge. The key idea behind our code design is to exploit the Sylvester structure of $\boldsymbol{C}_m$ in designing codes that satisfy (20). It turns out that there is a one-to-one mapping between the matrices $\boldsymbol{C}_m$ and their $\mathcal{Z}$-transform code polynomials $C_m(z) := \Sigma_{n=0}^{N_c-1} c_m(n) z^{-n}$. In particular, if ρ is a root of $C_m(z)$, one can verify by direct substitution that the Vandermonde vector $\boldsymbol{g}^T := [1 \rho^{-1} \cdots \rho^{-P+1}]$ is a left null-vector of the corresponding matrix $\boldsymbol{C}_m$, i.e., $\boldsymbol{g}^T \boldsymbol{C}_m = \boldsymbol{0}^T$. Hence, the null spaces of matrices $\{\boldsymbol{C}_m\}_{m=1}^{M}$ can be controlled by the roots of the corresponding polynomials $\{C_m(z)\}_{m=1}^{M}$. Based on these ideas, our code design algorithm follows these steps.

Step 1) Select a set of M distinct nonzero complex points $\{\rho_\mu\}_{\mu=1}^{M}$.

Step 2) Use ρ_μ's to construct M *Lagrange* polynomials (each of order $M-1$):

$$C_m(z) = A_m \frac{\prod_{\mu=1, \mu\neq m}^{M} (1 - \rho_\mu z^{-1})}{\prod_{\mu=1, \mu\neq m}^{M} (1 - \rho_\mu \rho_m^{-1})} \qquad m \in [1, M] \quad (21)$$

where A_m is a constant that controls the mth user's transmitted energy.

Step 3) Build the M *Vandermonde* receive filters $\boldsymbol{g}_\mu^T := [1\ \rho_\mu^{-1}\ \rho_\mu^{-2} \cdots \rho_\mu^{-P+1}]$.

By direct substitution, it follows that $C_\mu(\rho_\mu) = A_\mu$ and $C_m(\rho_\mu) = 0$ for $m \neq \mu$; hence

$$\boldsymbol{g}_\mu^T \boldsymbol{C}_m = [C_m(\rho_\mu), \rho_\mu^{-1} C_m(\rho_\mu), \cdots, \rho_\mu^{-L} C_m(\rho_\mu)] = \boldsymbol{0}^T \quad (22)$$

for $m \neq \mu$, whereas $\boldsymbol{g}_\mu^T \boldsymbol{C}_\mu = A_\mu [1 \rho_\mu^{-1} \rho_\mu^{-2} \cdots \rho_\mu^{-L}]^T \neq \boldsymbol{0}^T$; therefore, we have

$$\boldsymbol{g}_\mu^T \boldsymbol{C}_\mu \boldsymbol{h}_\mu = A_\mu \sum_{l=0}^{L} h_\mu(l) \rho_\mu^{-l} := A_\mu H_\mu(\rho_\mu) \quad \forall \mu \in [1, M]. \quad (23)$$

Root ρ_μ is not a root of $C_\mu(z)$ but is what we term a "signature root" for user μ because the Vandermonde receiver $\boldsymbol{g}_\mu^T$ employs ρ_μ in order to recover $s_\mu(n)$ and eliminate MUI interference that users $m \neq \mu$ introduce to user μ [by our design (21), ρ_m is a root of $\{C_\mu(z)\}_{\mu=1, \mu\neq m}^{M}$]. Note also that the pairs of LV transceivers obey, by construction, (20), and upon substituting (22) and (23) into (19), we obtain

$$\boldsymbol{g}_\mu^T \boldsymbol{x}(n) = A_\mu H_\mu(\rho_\mu) s_\mu(n) + \boldsymbol{g}_\mu^T \boldsymbol{v}(n). \quad (24)$$

In words, (24) shows that complete MUI cancellation is achieved deterministically and that each frequency-selective channel is converted to a scalar multiplicative factor (flat-fading coefficient) $H_\mu(\rho_\mu)$.

For minimum redundancy, $P = M + L$ and symbol periodic codes ($Q_c = 1 \Rightarrow N_c = M$), we will prove that the LV transceiver pair is the *only* one capable of accommodating exactly M users while achieving deterministic *channel-independent* MUI cancellation with a simple linear receiver (see Appendix A for the proof).

Proposition 1: Under a1)–a3), minimum spreading $P = M + L$ and minimum code length $N_c = M$ Lagrange precoders and Vandermonde receivers are the only MUI-free transceiver pairs. ■

Having established the uniqueness of LV pairs as the only MUI-free CDMA transceivers, we focus on special choices of the code roots. Already, from [24], one can recognize links of LV-CDMA with OFDMA, which correspond to choosing $\rho_m = \exp(j2\pi m/M)$. The next proposition not only solidifies this link but also attaches a means of optimality for such a choice of signature roots (see Appendix B for the proof).

Proposition 2: OFDMA with a prefix of zeros corresponds to the Lagrange codes and Vandermonde receivers using roots $\rho_i = \exp(j2\pi i/M)$, $i = 0, \cdots, M-1$. In this case, codes and receivers are matched, i.e., the mth Lagrange Vandermonde pair is $c_m(n) = \exp(j2\pi nm/M)$, and $g_m(n) = \exp(-j2\pi mn/M)$, $n = 0, \cdots, M-1$. ■

Interestingly, the MUI-free code design for quasisynchronous CDMA transmission in [19] can be interpreted as a special case of the OFDMA roots selection but with more than one signature root assigned to each user (see also Section VII-B). Of course, to enforce $MUI = 0$, different users have distinct sets of roots. The user's codes in [19] are a linear combination of the OFDMA codes polynomials with magnitude one coefficients. The code construction in [19], starts from the Rake receiver structure in (15), and the related discussion in Section II explains why MUI-free codes in [19] are such that $N_c = P \gg M$.

We will introduce next a dual VL pair equipped with the same MUI elimination capabilities. VL-CDMA transceivers will allow for an easier dynamic root assignment with advantages similar to power control techniques used in CDMA and the added feature of requiring minimal coordination among users.

IV. Vandermonde-Lagrange CDMA

From (24), we recall that LV transceivers eliminate MUI and convert the channel's frequency selectivity into flat fading. To cope with this residual flat fading effect, we can exploit the M degrees of freedom available with the location of the M roots ρ_i.

To simplify the process of switching from one code set to another and add flexibility to our system, we propose to interchange the roles of Lagrange with Vandermonde filters. We will show that the desired properties (22) and (23) are in effect even if we use Vandermonde precoders and Lagrange decoders. We will term the transceivers adopting this section's precoder-decoder structure VL transceivers. Specifically, given a set of roots $\{\rho_i\}_{i=1}^{M}$, we build the VL transceiver pairs as follows.

i) Precoder for the mth user is the Vandermonde $1 \times P$ vector $\boldsymbol{c}_m^T := A_m(\rho_m^{-P+1}, \cdots, \rho_m^{-1}, 1)$, where A_m is the power-controlling constant.

ii) Decoder for the μth user is the $1 \times P$ vector $\boldsymbol{g}_\mu^T := (0, \cdots, 0, \ell_\mu(M-1), \cdots, \ell_\mu(0))$, where $\ell_\mu(n)$ are the coefficients of the polynomial [c.f. (21)]

$$\mathcal{L}_\mu(z) := \frac{\prod_{m=1, m\neq\mu}^{M} (1-\rho_m z^{-1})}{\prod_{m=1, i\neq\mu}^{M} (1-\rho_m \rho_\mu^{-1})}, \qquad \mu \in [1, M]. \quad (25)$$

The leading zeros in $\boldsymbol{g}_\mu^T$ are used to cancel the guard interval where there is superposition of two consecutive symbols due to $\boldsymbol{C}_\mu(1) \neq \boldsymbol{0}$. Leading zeros in the VL design play the dual role of the trailing zeros inserted in the LV design to prevent ISI. In Appendix C, we prove the following.

Proposition 3: If $N_c = M + L$, the code/receiver design with minimum spreading $P = M + L$ corresponds to the dual VL transceiver pair. The conventional OFDMA scheme with cyclic prefix is the counterpart of the OFDM with trailing zeros (Proposition 2) in the VL design. ■

The advantage of the new formulation with respect to the LV design shows when a deep fade, say $H(\rho_m) = 0$, occurs. For example, if the mth channel has a zero on ρ_m, it is evident from (23) that the mth user cannot be recovered. Using power control, as foreseen by UMTS, for example, [15] would not help either because the received power would remain zero irrespective of the transmitted power. However, one can avoid the problem by replacing the root ρ_m with another root $\rho'_m \neq \rho_m$ under the premise that ρ'_m is unlikely to be a channel root. The BS then needs only to warn the mth transmitter to switch from root ρ_m to a different root, but all other users remain operational without changing roots. Hence, the new formulation increases the system's flexibility in the root assignment procedure. Of course, changing one user's root requires modification of all the decoder vectors, but this operation is performed at the BS; thus, VL is less troublesome than LV, where all the users have to change their precoders when changes occur.

V. Long-Codes and Multirate LV-CDMA Systems

Thus far, zero or negligible ISI was allowed in our designs. The received data block in the presence of ISI is given by (12). ISI can be either an undesired effect arising when the channel order exceeds the spreading factor ($L > P$) or an induced effect due to a code length $N_c > P$ spanning more than one symbol. From our discussion by the end of Section II, the minimum spreading necessary to achieve exact channel independent MUI cancellation is $P = M + L$, which is incompatible with the inequality $L > P$. Therefore, when ISI is due to $L > P$, ZF receivers may or may not exist, but either way, they are channel dependent. The situation is different when *long* codes (lasting for the duration of several symbols) are adopted. In this case, $N_c > P$ and $P \geq M + L$ are allowed. CDMA systems, such as IS-95, adopt codes that change from symbol to symbol in order to enhance the intercell interference mitigation with matched (e.g., RAKE) receivers. In fact, the codes of two users in neighboring cells cannot persist in having strong crosscorrelation due to the dynamic variation of the code. Similarly, codes spanning more symbols add degrees of freedom in the design, which allow us to suppress interference from neighboring cells through the gain of coherent integration. In fact, the energy from the desired user's signal at the receiver output grows as N_c^2, whereas the average interference contribution increases as N_c; hence, the bigger N_c is, the more effective interference rejection becomes. However, it is important to emphasize that residual ISI mitigation and spreading gain depends on P rather than N_c, and therefore, P should be large enough to ensure reliable symbol decisions. The channel-independent MUI suppression feature of the LV/VL transceivers can be easily extended to systems utilizing long codes. A straightforward generalization of the LV/VL designs for $N_c > P$ that maintains minimum spreading $P = M + L$ is to adopt as users' codes $\boldsymbol{C}_m(q) = \alpha_m(q)\boldsymbol{C}_m$ and receivers $\boldsymbol{g}_m^T(k) = \gamma_m(k)\boldsymbol{g}_m^T$, for $k = 0, \cdots, Q_g - 1$.

With respect to the code $\boldsymbol{c}_m^{(0)} := \boldsymbol{c}_m$ of Sections III or IV, the code $\boldsymbol{c}_m^{(Q_c-1)}$ that now spans $Q_c > 1$ symbols and leads to $\boldsymbol{C}_m(q) = \alpha_m(q)\boldsymbol{C}_m$ is given by

$$\boldsymbol{c}_m^{(Q_c-1)} = \boldsymbol{\alpha}_m^{(Q_c-1)} \otimes \boldsymbol{c}_m^{(0)} \quad (26)$$

where $\otimes$ denotes the Kronecker product, and $\boldsymbol{\alpha}_m^{(Q_c-1)} := (\alpha_m(0), \cdots, \alpha_m(Q_c-1))^T$ is an arbitrary vector. In this case, (12) becomes

$$\boldsymbol{x}(n) = \sum_{m=1}^{M} \boldsymbol{C}_m \boldsymbol{h}_m \sum_{q=0}^{Q_c-1} \alpha_m(q) s_m(n-q) + \boldsymbol{v}(n) \quad (27)$$

and perfect MUI cancellation can be obtained along the lines described in Sections III and IV, provided that codes and receivers are designed to satisfy (20). With receiver structure $\boldsymbol{g}_m^T(k) = \gamma_m(k)\boldsymbol{g}_m^T$, MUI is canceled thanks to (20), and we obtain, for the mth user's symbol estimate

$$\hat{s}_m(n) = \boldsymbol{g}_m^T \boldsymbol{C}_m \boldsymbol{h}_m \sum_{k=0}^{Q_g-1} \sum_{q=0}^{Q_c-1} \gamma_m(k)\alpha_m(q) s_m(n+k-q) + \sum_{k=0}^{Q_g-1} \gamma_m(k)\boldsymbol{g}_m^T \boldsymbol{v}(n+k). \quad (28)$$

Different $\alpha_m(k)$ can be used in different cells to gain over the interfering signals. The coefficients $\gamma_m(k)$ depend on the strategy we adopt to cope with the deterministic ISI introduced by the long codes. Notice that contrary to $h_m(l)$, the coefficients $\alpha_m(q)$ are known to the receiver, and the two sequences $\alpha_m(q)$ and $\gamma_m(k)$ can be chosen in order to minimize ISI if their cross-correlation satisfies $R_{\alpha_m,\gamma_m}(k) := \sum_q \alpha_m^*(q)\gamma_m(k+q) \simeq R_{\alpha,\gamma}\delta(k)$. If $\alpha_m(k)$ are samples of a pseudo-noise sequence, the latter can be achieved with simple matched filtering $\gamma_m(k) = \alpha_m^*(k)$. For example, different cells may have different PN sequences. With $\boldsymbol{\eta}(n)$ denoting the colored noise term, (28) is given approximately by

$$\begin{aligned}\hat{s}_m(n) &\approx \boldsymbol{g}_m^T \boldsymbol{C}_m \boldsymbol{h}_m \sum_{q=0}^{Q_c-1} \delta(k-q) s_m(n+k-q) + \boldsymbol{\eta}(n) \\ &= \boldsymbol{g}_m^T \boldsymbol{C}_m \boldsymbol{h}_m s_m(n) + \boldsymbol{\eta}(n). \end{aligned} \tag{29}$$

If Q_g is not sufficiently large to assure $R_{\alpha_m,\gamma_m}(k) \simeq \delta(k)$, a precomputable linear MMSE Wiener receiver or a DFE can be adopted to achieve performance better than the matched filter receiver.

This coding strategy is also useful for CDMA systems because it enables different symbol rates through the assignment of heterogeneous spreading factors P_m. In the UMTS standard, all users employ the same chip rate, but the spreading factor P_m varies from 4 to 256 to accommodate users with different rates. The spreading codes are the Walsh–Hadamard basis vectors with length $N_c = 2^Q$ and are recursively generated through Q Kronecker products of all possible Qth-order permutations of the factors (1, 1) and (1, -1). These codes are constructed to be orthogonal for variable spreading factors (OVSF). Indeed, if there are two users A and B with a ratio between their symbol rates $N_{c,A}/N_{c,B} = P_A/P_B = 2^k$, their perfectly synchronous signals will be orthogonal to each other whenever user A code, with the greater spreading factor and code length, is generated as the Kronecker product of one of the $P_B - 1$ codes orthogonal to user B code, followed by 2^k arbitrary factors (1, 1) and (1, -1). Otherwise stated, the short code should not be a *parent* of any longer code. Assigning a code excludes all the subtrees (and possible users) originating from it, which implies that the number of possible OVSF codes and, consequently, users is limited by the number of users with highest rate/smallest spreading factor. Recall now that code orthogonality is lost in the presence of users' asynchronism and/or multipath propagation. Implanting the OVSF property to our LV-VL designs will follow the construction of the Walsh-Hadamard codes and the basic idea underlying (26)–(28). Assume w.l.o.g. that P_0 is the smallest spreading factor, corresponding to the highest possible rate. The number of highest rate users that can be accommodated with their LV-VL transceivers offering MUI suppression is $M_0 = P_0 - L$. However, similar to (26), from each code $\boldsymbol{c}_k^{(0)}$, $k = 1, \cdots, M_0$, we can generate Q_m distinct codes with various spreading factors $P_m = Q_m P_0$, allowing channel independent MUI elimination, as follows:

$$\boldsymbol{c}_m^{(Q_m-1)} = \boldsymbol{\alpha}_m^{(Q_m-1)} \otimes \boldsymbol{c}_{k_m}^{(0)}. \tag{30}$$

Vectors $\boldsymbol{\alpha}_m^{(Q_m-1)} = (\alpha_m(0), \cdots, \alpha_m(Q_m-1))^T$ are such that for all $Q_\mu = Q_m$, we have $\boldsymbol{\alpha}_\mu^T \boldsymbol{\alpha}_m = 0$. For a given $\overline{P} = \overline{Q} P_0$, we can define $\overline{Q}$ orthogonal codes $\boldsymbol{\alpha}^{(\overline{Q}-1)}$ and thus accommodate as many as $\overline{Q}$ users. As with the Walsh–Hadamard basis, to add flexibility to the system and allow for a wider variety of rates, $\boldsymbol{\alpha}_m^{(Q_m-1)}$ should also be chosen to satisfy the OVSF property. Hence, corresponding to one out of M_0 subcodes $\boldsymbol{c}_k^{(0)}$, there are all the possible users associated with the OVSF scheme relying on super-codes $\boldsymbol{\alpha}_m^{(Q_m-1)}$ for user separation. With the Walsh–Hadamard codes, a super-code with smaller rate cannot be parent of a super-code associated with the same subcode of a larger rate. Therefore, the number of possible users grows proportional to M_0 by a factor that varies from $\min_m Q_m$ and $\max_m Q_m$; thus, our system can support at least M_0 and at most $M_0 Q_{\max}$ MUI-free users with $Q_{\max}$ as the maximum possible spreading factor/lowest rate. In this case, assuming $P = P_0$ in all vector definitions for $q \in [0, Q_m - 1]$, (12) reduces to

$$\begin{aligned}\boldsymbol{x}(nQ_m + q) = &\sum_{m=1}^{M} \boldsymbol{C}_{k_m} \boldsymbol{h}_m \alpha_m(q) s_m(n) \\ &+ \boldsymbol{v}(n), \qquad q = 0, \cdots, Q_m - 1. \end{aligned} \tag{31}$$

Equation (31) is a further simplification of (27) with $s_m(n)$ being replaced by $\zeta_m(n) = \Sigma_k\, s_m(k)\delta(n - kQ_m)$, which is the mth user's symbol stream upsampled by a factor Q_m to achieve the highest rate $P = P_0$. We use the suffix k_m to indicate that the μth and mth users can have $k_m = k_\mu$, or in other words, they can have the same subcode. Derivation of the corresponding mth user's receiver is straightforward to find by setting

$$\boldsymbol{g}_m(q) = \alpha_m^*(q) \boldsymbol{g}_m, \qquad q \in [0, Q_m - 1]. \tag{32}$$

For equal subcodes $k_m = k_\mu$, since $\boldsymbol{g}_{k_m}^T \boldsymbol{C}_{k_\mu} = \delta(k_m - k_\mu) = 1$, the user separation is obtained trough the orthogonality between $\boldsymbol{\alpha}_m^{(Q_m-1)}$ and $\boldsymbol{\alpha}_\mu^{(Q_\mu-1)}$; hence, users operating at the same rate can use the same subcode. In fact

$$\begin{aligned}\hat{s}_m(n) &= \sum_{q=0}^{Q_m-1} \alpha_m^*(q) \boldsymbol{g}_{k_m}^T \boldsymbol{x}(nQ_m + q) \\ &= \boldsymbol{g}_{k_m}^T \boldsymbol{C}_{k_m} \sum_{\mu: k_\mu = k_m} \boldsymbol{h}_\mu \sum_{q=0}^{Q_m-1} \alpha_m^*(q) \alpha_\mu(q) s_\mu(n) \\ &\quad + \sum_{q=0}^{Q_m-1} \alpha_m(q) \boldsymbol{g}_{k_m}^T \boldsymbol{v}(n+q) \\ &= \boldsymbol{g}_{k_m}^T \boldsymbol{C}_{k_m} \boldsymbol{h}_m \sum_{q=0}^{Q_m-1} |\alpha_m(q)|^2 s_m(n) \\ &\quad + \sum_{q=0}^{Q_m-1} \alpha_m(q) \boldsymbol{g}_{k_m}^T \boldsymbol{v}(n+q). \end{aligned} \tag{33}$$

Equation (33) shows that the LV/VL-CDMA system eliminates MUI while allowing heterogeneous symbol rates, which is a property not exhibited by the OVSF Walsh–Hadamard basis code vectors.

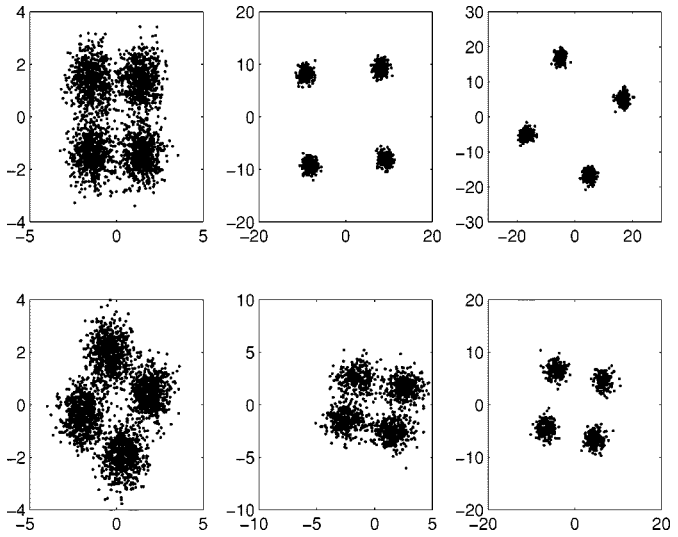

Fig. 2. Scattering diagrams with the LV transceivers for $N_c = 6, 12, 18$.

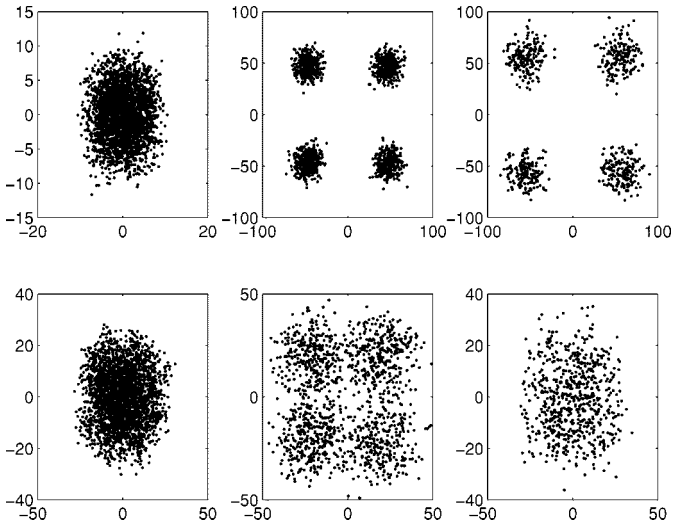

Fig. 3. Scattering diagrams with OVSF Walsh–Hadamard codes and RAKE for $N_c = 4, 8, 16$.

Example 1—Users with Multiple Rates: We compare our multirate LV transceivers against OVSF codes processed by a RAKE receiver that assumes perfect knowledge of the channel. In both cases, two users at three different rates are simultaneously active. The SNR is 20 dB for both systems. The channels are generated randomly as FIR filters of order $L = 2$ with taps that are complex Gaussian variables with variance $\sigma^2_{h_m(l)} = 1$. The same set of channels is used in both schemes. The codes have been selected so that shorter codes are not *parents* of longer codes in order to guarantee users' orthogonality, at least under ideal propagation conditions. From the scattering diagrams in Figs. 2 and 3 (different rows and columns refer, respectively, to different users and code lengths), we infer that although long Hadamard codes manage to recover from MUI, this is not true for short codes. Moreover, robustness with respect to fading is traded with a consistent degradation in performance due to MUI. Notice also that since the LV receiver is MUI free, it clearly outperforms the RAKE receiver.

VI. Performance Analysis

In all MUI-free schemes examined so far, the multipath channel $\boldsymbol{h}_m$ affects the mth user's performance through the flat fading factor $\boldsymbol{g}_m^T \boldsymbol{C}_m \boldsymbol{h}_m = A_m H_m(\rho_m)$. Symbol recovery requires mitigation of the multiplicative constant $H_m(\rho_m)$ in

$$\boldsymbol{g}_m^{\mathcal{H}} \boldsymbol{x}(n) = A_m H_m(\rho_m) s_m(n) + \boldsymbol{g}_m^{\mathcal{H}} \boldsymbol{v}(n) \tag{34}$$

which amounts to either estimating and removing $H_m(\rho_m)$ or decoding via differential demodulation the differentially encoded symbols. In both cases, channel variations are not allowed to be as fast as the symbol rate.

Statistical characterization of $H_m(\rho_m)$ follows easily from the distribution of the channel vector $\boldsymbol{h}_m$ since

$$H_m(\rho) := \sum_{l=0}^{L} h_m(l) \rho^{-l} = \boldsymbol{\rho}^T \boldsymbol{h}_m \tag{35}$$

where $\boldsymbol{\rho} := (1 \rho_p^{-1} \rho_p^{-2} \cdots \rho_p^{-L})^T$. Probability of error for the mth user depends on the signal-to-noise ratio (SNR) (SNR_m) at the output of the $g_m(n)$ filter. If we normalize the spreading-code energy, it is not difficult to prove that the LV and VL codes achieve exactly the same performance in terms of SNR_m^{ZF}, which denotes the mth user's SNR at the output of the ZF receiver. Let us assume first that we adopt the LV scheme of Section III. Because $\boldsymbol{v}(n)$ is an AWGN vector, the noise term in (34), becomes a (generally colored) Gaussian random variable with zero mean and variance

$$E\{|\boldsymbol{g}_m^T \boldsymbol{v}(n)|^2\} = \sigma_v^2 \boldsymbol{g}_m^{\mathcal{H}} \boldsymbol{g}_m = \sigma_v^2 \frac{1 - |\rho_m|^{-2P}}{1 - |\rho_m|^{-2}}. \tag{36}$$

Based on (34) and (36), SNR_m^{ZF} is given by

$$\begin{aligned} \text{SNR}_m^{ZF} &:= \frac{\sigma_s^2(m) |\boldsymbol{g}_m^T \boldsymbol{C}_m \boldsymbol{h}_m|^2}{\sigma_v^2 \boldsymbol{g}_m^H \boldsymbol{g}_m} \\ &= \frac{\sigma_s^2(m) |A_m|^2 (1 - |\rho_m|^{-2})}{\sigma_v^2 (1 - |\rho_m|^{-2P})} |H_m(\rho_m)|^2 \\ &:= \alpha_m |H_m(\rho_m)|^2 \end{aligned} \tag{37}$$

where $\sigma_s^2(m)$ is the mth user's received power. In the VL case, normalizing the Vandermonde spreading code introduces the factor $(1 - |\rho_m|^{-2})(1 - |\rho_m|^{-2P})$, whereas the term $|A_m|^2$ at the numerator of (37), which normalizes the Lagrange polynomials, is due to $1/(\boldsymbol{g}_m^{\mathcal{H}} \boldsymbol{g}_m)$, that is, the inverse of the Lagrange receivers' energy. Hence, (37) with $A_m := \Sigma_{n=0}^{M-1} |\ell_m(n)|^2$ is valid for both LV and VL schemes.

If, instead of the Vandermonde (Lagrange) receiver, the Rake receiver $\boldsymbol{g}_m^T = \boldsymbol{h}_m^{\mathcal{H}} \boldsymbol{C}_m^{\mathcal{H}}$ is adopted, the interference from the other users will increase the noise power, and the SNR_m^{MF} will be

$$\begin{aligned} \text{SNR}_m^{MF} &:= \frac{\sigma_s^2(m) |\boldsymbol{g}_m^{\mathcal{H}} \boldsymbol{C}_m \boldsymbol{h}_m|^2}{\sigma_v^2 \boldsymbol{g}_m^H \boldsymbol{g}_m + \sigma_{MUI}^2(m)} \\ &= \frac{\sigma_s^2(m) \boldsymbol{h}_m^{\mathcal{H}} \boldsymbol{C}_m^{\mathcal{H}} \boldsymbol{C}_m \boldsymbol{h}_m}{\sigma_v^2 + \sigma_{MUI}^2(m) / (\boldsymbol{h}_m^{\mathcal{H}} \boldsymbol{C}_m^{\mathcal{H}} \boldsymbol{C}_m \boldsymbol{h}_m)} \end{aligned} \tag{38}$$

where $\sigma^2_{MUI}(m)$ denotes the power of the MUI at the output of the mth user's receiver. Assuming that the users are uncorrelated, the latter is given by

$$\sigma^2_{MUI}(m) = \sum_{\mu=1,\mu\neq m}^{M} |\boldsymbol{h}_m^{\mathcal{H}} \boldsymbol{C}_m^{\mathcal{H}} \boldsymbol{C}_\mu \boldsymbol{h}_\mu|^2 \sigma_s^2(\mu). \quad (39)$$

Modeling the interference at the output of the Rake receiver as a zero mean Gaussian random variable, the probability of error at the output of the Rake will be completely determined by (38). Therefore, depending on the number of active users and relative power levels, one may select either the ZF receiver that is MUI free and does not suffer from near-far effects or the Rake receiver, which is fading resistant. When the number of users approaches $P = M + L$, most users will find it convenient to switch to the ZF mode.

A. Outage Probability

Differential encoding and decoding offers simplicity at the expense of performance loss in terms of bit error rate (BER) (see e.g., [2]). The alternative is frequent retraining to track channel variations, which reduces bandwidth efficiency prohibitively, especially when rapid variations are present. In such cases, a channel independent MUI receiver followed by differential demodulation is well motivated. Under the AGN assumption, noncoherent detection based on (34) for differential (D-)BPSK incurs probability of error [2]:

$$P_e(\rho_m, \boldsymbol{h}_m) = \tfrac{1}{2} \exp(-\mathrm{SNR}_m). \quad (40)$$

In the coherent case, error probability is proportional to $\mathrm{erfc}(x)$, where x depends on $\mathrm{SNR}^{1/2}$ with proportionality factors that are constellation specific. Because, for $x \gg 1$, $\mathrm{erfc}(x) < \exp(-x^2)$, we can adopt the approximation $\mathrm{erfc}(x) \approx \exp(-x^2)$ and scale properly the exponential argument to infer that (40) can still serve us as an upper bound.

To assess performance further, we model the mth unknown fading channel as a complex Gaussian random vector $\boldsymbol{h}_m$ with zero-mean independent components (which corresponds to the widely used Rayleigh fading model arising when no direct path arrives at the receiver [16]). The exponential distribution is approximately valid, even when the coefficients $h_m(l)$ are non-Gaussian, provided that the following extra conditions are met: i) the number of paths is sufficiently large; ii) the $h(\mu)$'s have finite moments (which is certainly true in practice) and are weakly correlated. Hence, $H_m(\rho_m)$ in (35) is also a zero mean complex Gaussian random variable and conditioned on $\sigma_s^2(m)$, which implies that $\mathrm{SNR}_m = \mathrm{SNR}_m^{ZF} = \alpha_m |H_m(\rho_m)|^2$ follows an exponential distribution $p_{\mathrm{SNR}_m^{ZF}}(s) = 1/\overline{\mathrm{SNR}}_m^{ZF} \exp(-s/\overline{\mathrm{SNR}}_m^{ZF})$, with

$$\overline{\mathrm{SNR}}_m^{ZF} = \alpha_m \sigma^2_{H_m(\rho_m)} = \alpha_m \boldsymbol{\rho}_m^{\mathcal{H}} \boldsymbol{R}_{h_m} \boldsymbol{\rho}_m \quad (41)$$

where $\boldsymbol{R}_{h_m}$ is the channel covariance matrix.

With ρ_m corresponding to the mth receiver, the mean $P_e(\rho_m, \boldsymbol{h}_m)$, averaged over all possible channels, is proportional to the characteristic function of SNR_m, and for the ZF receiver, we obtain

$$E_{\boldsymbol{h}_m}\{P_e^{ZF}(\rho_m, \boldsymbol{h}_m)\} = \frac{1}{2} E\{\exp(-\mathrm{SNR}_m^{ZF})\} = \frac{1}{2} \frac{1}{1 + \overline{\mathrm{SNR}}_m^{ZF}}. \quad (42)$$

However, the average $P_e(\rho_m, \boldsymbol{h}_m)$ alone is not fully representative of the overall system performance because there may be great variations in $P_e(\rho_m, \boldsymbol{h}_m)$. To characterize completely $P_e(\rho_m, \boldsymbol{h}_m)$ and provide a practical figure of merit, we computed the outage probability $P_{out}(\mathcal{T})$, which is defined as the probability that $P_e(\rho_m, \boldsymbol{h}_m) > \mathcal{T}$, where $\mathcal{T}$ is the maximum tolerable error probability that depends on the quality of service. A system is declared *out of service* if the error probability exceeds a prescribed threshold, e.g., for speech $\mathcal{T} = 10^{-3}$; therefore, $P_{out}(\mathcal{T})$ gives the percentage of time over which the system is considered out of service for the given $\mathcal{T}$.

The closed-form expression of $P_{out}(\mathcal{T})$ is[5]:

$$P_{out}(\mathcal{T}) := \Pr\{P_e^{ZF}(\rho_m, \boldsymbol{h}_m) > \mathcal{T}\} = 1 - (2\mathcal{T})^{1/\overline{\mathrm{SNR}}_m^{ZF}}. \quad (43)$$

Thanks to the code/receiver design, $P_{out}(\mathcal{T})$ in (43) does not depend on power control or the number of users; thus, although simple to compute, it is a very useful link-reliability parameter.

Example 2—Lagrange versus OFDMA for Time-Invariant Channels: To test Lagrange versus OFDMA coding strategies, we simulated $M = 16$ users with roots $\{\rho_m = [1 + 0.1\cos(\pi m/2)] \exp(j2\pi m/M)\}$, with $m = 0, \cdots, M-1$, shown in Fig. 4 with circles, along with OFDMA's root constellation ('+'). We assumed the channel covariance matrix to be $\sigma_h^2 \boldsymbol{I}$, with σ_h^2 constant for all channels, the same transmitted energy per bit for all users, and channel order $L = 4$. The outage probability versus E_b/N_0 is depicted in Fig. 5, where N_0 is the receiver-noise power spectral density. The outage probability of the LV scheme with signature roots

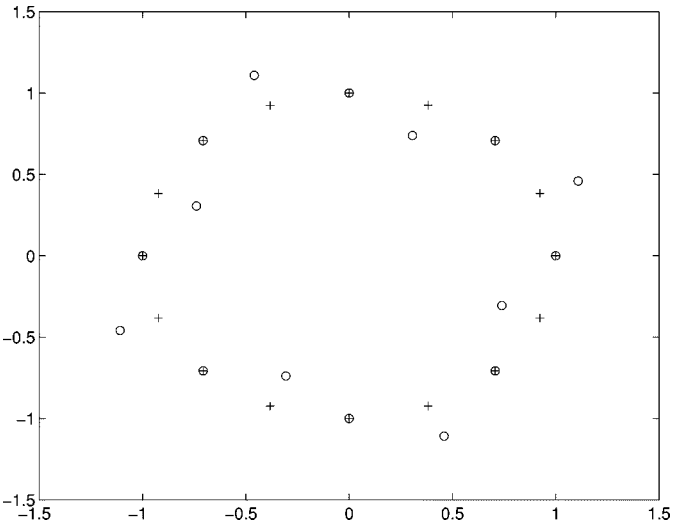

Fig. 4. Roots of user codes.

[5]Using (40) $\Pr\{P_e^{ZF}(\rho_m, \boldsymbol{h}_m) > \mathcal{T}\} = \Pr\{\mathrm{SNR}_m < -\log \mathcal{T}\}$. The last can be easily computed from the exponential distribution of SNR_m.

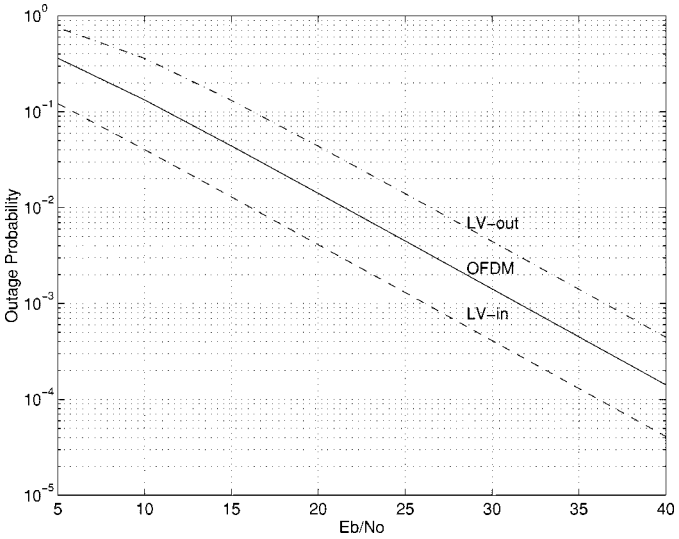

Fig. 5. Outage probability versus E_b/N_0; OFDMA (dashed line) LV users with roots inside (LV-in dashed) and outside (LV-out dash-dotted).

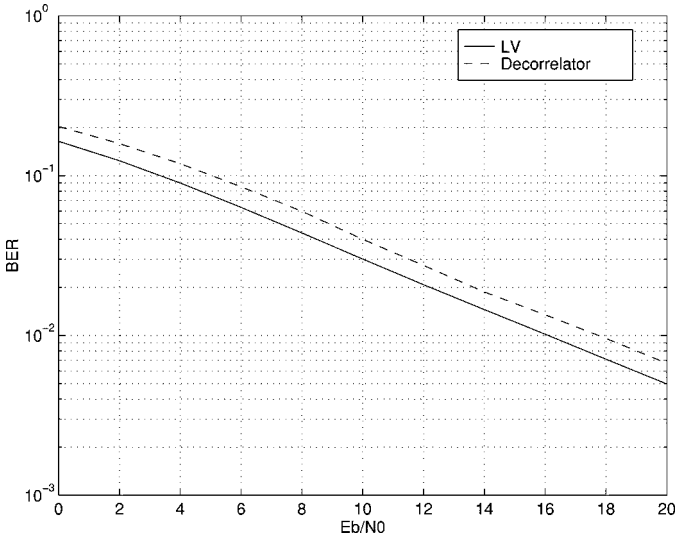

Fig. 6. BER versus E_b/N_0 for LV and Walsh-Hadamard and Decorrelating receiver in a asynchronous flat fading scenario ($L = 1, P = 32+L, M = 16$).

depicted in Fig. 4 varies, depending on the root position relative to the unit circle, whereas it remains constant for OFDMA (dashed line). Lower P_{out} is achieved for the users whose code roots have maximum amplitude 1.1, whereas those having amplitude 0.9 have P_{out} higher than OFDMA whose performance is in the middle (and coincides with the performance of the roots with amplitude 1). This feature is potentially useful when the system is desired to accommodate different priority users.

The best average performance in a purely frequency selective scenario and, with arbitrary root assignment, is achieved with the OFDMA scheme. However, a first advantage of the extra degrees of freedom offered by the LV/VL designs arises if we consider also time selectivity effects, which constitute the main drawback of OFDMA schemes as will be shown in the ensuing section.

Example 3—Comparison with Decorrelating and Rake Receivers: The *delay-independent* receiver in [7] has low complexity, as does our design. For the flat-fading QS scenario offers a suboptimal low complexity implementation of the decorrelating receiver in [13].

Relative to our frequency-selective channels, the channels in [7] correspond to pure delays, and if L is the maximum delay in terms of chips, in order to have $MUI = 0$, the receiver in [7] requires $P = M(L+1) + L$, with a capacity loss around 50% for a single delay chip. Thanks to our judicious code design, the LV transceivers can also cope with Lth-order multipath channels with minimal spreading $P = M + L$. As we saw in Section II, if the channel is a pure delay times, a fading scaling constant $h_m(l) = \alpha_m R_{\phi\phi}(lT_c - \tau_m)$. Since $R_{\phi\phi}(t)$ is a Nyquist pulse, the channel transfer function will be basically flat by construction. Assuming Hadamard codes with zero guard time, setting $M = 32$ and $L = 1$, we consider 16 active users with spreading codes numbered as $2i+1$ with $i \in [0, 15]$, as in [7, Tab. I]. From Fig. 6, we observe that OFDMA outperforms the *delay-dependent* decorrelating receiver in [13] (and, thus, it's also the delay-independent version of [7]) in terms of average BER (over 100 fading channel realizations). The users' channels are $h_m(l) = \alpha_m R_{\phi\phi}(lT_c - \tau_m)$, with τ_m uniformly

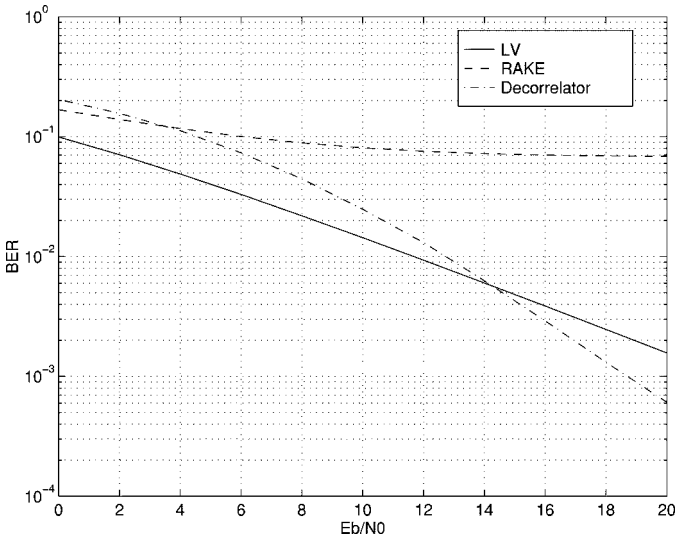

Fig. 7. BER versus E_b/N_0 for LV and Gold codes of length 127 and decorrelating receiver in frequency-selective fading ($L \approx 15, P = 127, M = 100$).

distributed over one chip period, and $R_{\phi\phi}(t)$ is the raised-cosine chip-pulse with roll-off 0.22 (the rectangular pulses were used in [7]).

In the presence of frequency selectivity our scheme suffers on the average from fading. The average BER curves in Fig. 7 are obtained for 100 active users with Gold codes, $P = N_c = 127$, and a six-finger RAKE receiver (dashed line) or the decorrelating receiver of [13] (dashed dotted line). For our design (solid line), we used 100 roots placed uniformly around the unit circle. The random channels are generated using the power-delay profile known as Vehicular-B [15]; we assumed, as in UMTS [15], a chip rate of 4096 $Mcps$ that the delays are τ = [0, 0.25, 0.5, 0.75, 1, 1.2, 1.7, 1.9, 2.4, 2.7] μs and that the paths' amplitudes are complex uncorrelated Gaussian random variables with zero mean and variance [0, −2.5, −6.5, −9.5, −12.5, −13, −15.5, −25.5, −21.5, −25.5] dB's; a raised-cosine chip pulse

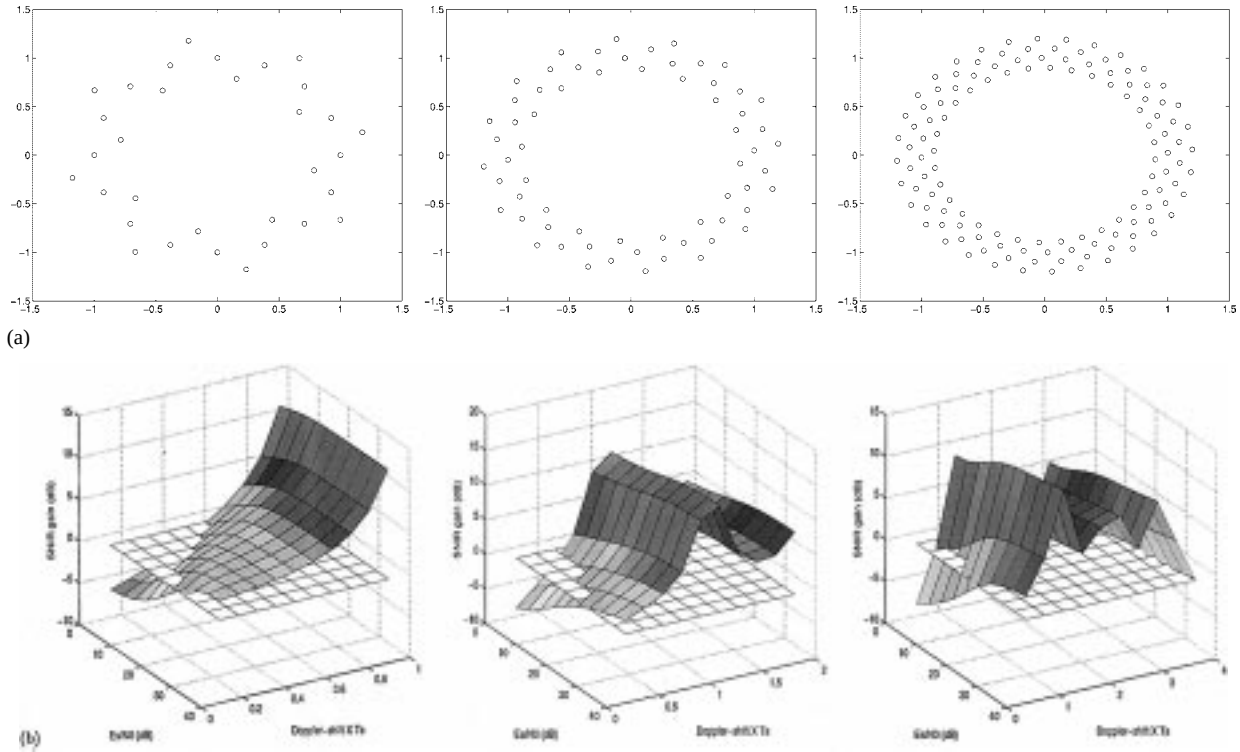

Fig. 8. (a) Roots of user codes for $M = 32, 64, 128$. (b) SNIR gain: Lagrange versus OFDMA for $M = 32, 64, 128$, respectively.

with roll-off 0.22 was used and the resulting random channel orders $L \in (11, 15)$. Hence, appending 27 zeros to our 100-long codes, our spreading factor $P = 127 > M + L$. In these cases, at high SNR, the decorrelating receiver outperforms the OFDMA solution. However, the decorrelator requires estimation of $\approx (L+1)M = 2048$ channel taps and the inversion of a matrix of size 100. Furthermore, there is no guarantee that the ZF receiver exists for all possible channels.

B. Doppler Effects

In contrast to OFDMA, where code roots are fixed and equispaced around the unit circle, root locations in LV-CDMA can be optimized to improve performance when dealing with frequency- and time-selective channels. Time selectivity arising due to Doppler effects and/or carrier offsets manifests itself as multiplicative $\exp(j\omega_m n)$ factors, modulating each of the channels $h_m(l)$. The μth receiver output then becomes

$$\begin{aligned}\boldsymbol{g}_\mu^{\mathcal{H}}\boldsymbol{x}(n) = {} & s_\mu(n)e^{j\omega_\mu nP}H_\mu(\rho_\mu e^{-j\omega_\mu})C_\mu(\rho_\mu e^{-j\omega_\mu}) \\ & + \boldsymbol{g}_\mu^{\mathcal{H}}\boldsymbol{v}(n) \\ & + \sum_{m\neq\mu} s_m(n)e^{j\omega_m nP}H_m(\rho_\mu e^{-j\omega_m})C_m(\rho_\mu e^{-j\omega_m})\end{aligned} \tag{44}$$

which shows that three undesired effects arise.

ii) Symbols are modulated by $\exp(j\omega_m nP)$.

iii) Channel and code roots rotate by the *unknown* angle ω_m on the complex plane.

iv) MUI is superimposed to the user of interest because ρ_μ is no longer a common root of $\{C_m(ze^{-j\omega_m})\}_{m=1,m\neq\mu}^{M}$ (roots of the latter have rotated by ω_m).

The signal-to-noise and interference ratio (SNIR) for the μth user, resulting from (44), can be easily found to be (45), shown at the bottom of the page. Therefore, at least in principle, user codes can be designed to maximize SNIR_μ, $\forall\mu$ by optimizing code root locations. The optimization is challenging because SNIR_μ depends nonlinearly on ρ_μ. However, suboptimal codes increasing robustness against frequency drifts can be devised by designing polynomials $C_m(z)$ such that i) $C_\mu(\rho_\mu e^{-j\omega_\mu})$ is as flat as possible $\forall\mu$, and ii) $C_m(\rho_\mu e^{-j\omega_m})$ is as small as possible $\forall m \neq \mu$.

Example 4—Time-Selective/Doppler Effects: To test our Lagrange codes, we simulated $M = 32, 64, 128$ users with the roots located on concentric circles (each time 25% of the users have their signature roots on circles with radius $|\rho| = 1.2, 1.1, 0.9, 0.8$). We also compared LV with OFDMA, which assigns signature roots of all users on the unit circle. Fig. 8(b) depicts the ratio between $SNIR_m^{LV}/SNIR_m^{OFDMA}$

$$\text{SNIR}_\mu = \frac{|H_\mu(\rho_\mu e^{-j\omega_\mu})|^2|C_\mu(\rho_\mu e^{-j\omega_\mu})|^2}{\left[\sum_{m\neq\mu}^{M}|H_m(\rho_\mu e^{-j\omega_m})|^2|C_m(\rho_{mu}e^{-j\omega_m})|^2 + \sigma_v^2(1-|\rho_\mu|^{-2P})/(1-|\rho_\mu|^{-2})\right]}. \tag{45}$$

obtained with the LV and OFDMA systems as a function of the SNR and the frequency shift, normalized to one symbol interval $f_m T_s$. The energy of users' codes is normalized, in all cases, to 1. Channel taps $h_m(n)$ were generated as independent Gaussian random variables to simulate Rayleigh fading channels of order $L = 5$. Fig. 8(b) depicts the SNIR gain (in decibels) averaged over 128 independent channel realizations per user and over the M users and shows that OFDMA yields better performance for very small frequency shifts and at low SNR. However, as soon as the frequency shift exceeds a small fraction of the OFDMA filter bandwidth $1/T_s$, the LV schemes built from the roots of Fig. 8(a) outperform OFDMA. In particular, for $M = 128$, the SNIR gain goes to zero when the product $f_m T_s = 4$, and this is due to the fact that the angle that separates the signature roots of the LV scheme in this particular case is four times the spacing between the OFDMA roots, which is $2\pi/128$. Unfortunately, the severe interference causes the corresponding BER curves to be very high for both schemes, and the differences in performance are then less accentuated than in the SINR gain curves.

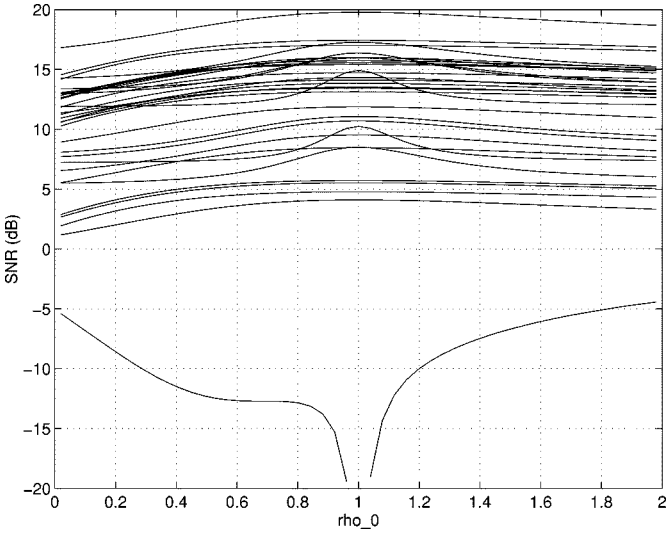

Fig. 9. Power received from all 32 users versus the modulus of the root of the user with a deep fade.

VII. Fading Resistant LV/VL Variants

To cope with the residual flat fading effects, in this section we describe nonredundant and redundant (diversity-enhanced) modifications of our basic LV/VL design.

A. Root versus Power Control

For a given set of channels, the degrees of freedom offered by the root selection could be optimally exploited by searching for the set of roots that minimize the error probabilities of all users. However, even for known channels, such an optimization requires nonlinear programming with a large number of parameters. Furthermore, the proposed LV/VL transceivers guarantee zero-MUI, irrespective of the channel zero locations and without channel status information (CSI). In this subsection, we propose a nonredundant suboptimal technique for changing the root positions when deep fades occur while maintaining the blind capability of our transceivers. The method generalizes the power control technique currently foreseen by UMTS, where the BS sounds the power level of the signals received from all active users and sends back control signals requiring users to increase or decrease their transmitted power in order to limit MUI. In principle, the LV/VL coding strategy eliminates MUI completely so that power control is not needed to attenuate interference. However, some procedure must be developed to recover from deep fades that arise when some channels have zeros at the corresponding users' codes.

With M denoting the maximum number of active users the BS starts working with a set of complex roots equispaced around the unit circle as with OFDMA. Proposition 2 established that for flat fading channels, OFDMA maximizes SNR because the decoder is a filter matched to the precoder. With each user's signature root on the unit circle, the BS periodically sounds the power received from all active users. If some users are received with a power below a prescribed threshold, the BS initializes a procedure to move the corresponding root away from its initial position. If the number of active users is less than the maximum number of users, the BS may simply assign a new signature root on the unit circle to a low-power user. However, if the unit-circle roots are all occupied because the number of active users is equal to its maximum value, the BS must undertake a different action. Different from OFDMA, where the root positions are fixed, in our VL-CDMA system, the BS moves the root of the deeply faded user radially on the complex plane (the root's phase is not altered to avoid undesired coincidence with other roots), varying its modulus within a certain range. The user thus gets assigned a new signature root having the same angle as before but with the modulus corresponding to the maximum power received from the BS. If that power level is still insufficient for reliable decoding, the BS requests from the user to increase the transmitted power.

Example 5—VL with Root Control: Fig. 9 refers to a CDMA system where 32 possible users are all active, and one of them (say, the user corresponding to the root $\rho = 1$) transmits through a channel having a zero at $z = 1$. Power control can not handle such a fading effect. Fig. 9 shows the power that the BS receives from all users as a function of the signature root of the user experiencing the deep fade (each user transmits at a level of 0 dBW). We observe that for $\rho = 1$, the power received from one user goes to $-\infty$ dB. Changing the root location, some of the other users will suffer some loss, but the user with the deepest fade will recover. This gain is not possible by adjusting only the user's transmit power. After having recovered from the deep fade, further power control may be used to balance the relative power among different users.

We also considered a system with 64 users, and we simulated two users' channels to have zeros on the corresponding users' codes. The BS changes the position of all users such that the corresponding received power falls below a prescribed level. Fig. 10 shows the final position of the roots (the '+' correspond to the initial position, whereas the 'o' correspond to the final position). With E_b denoting the energy per bit and N_0 the noise

power spectral density, the minimum ratio E_b/N_0 recovers from $-\infty$ dB to -7 dB.

B. Redundancy Against Fading

From (22) and (23), we recall that the VL scheme eliminates MUI and converts frequency-selective fading channels into flat fading channels characterized by the complex factor $H_\mu(\rho_\mu)$. This factor may cause severe attenuation if ρ_μ is equal (or close) to a root of $H_\mu(z)$. To improve the robustness of the VL scheme, we may assign extra signature roots to each user. Specifically, if we assign Q signature roots to each user and associate Q Vandermonde vectors with each transmitted symbol $s_\mu(n)$, the signal received by the μth receiver is

$$\boldsymbol{x}_\mu(n) = \sum_{m=1}^{M} \sum_{q=1}^{Q} \boldsymbol{C}_{m,q} \boldsymbol{h}_m s_m(n) + \boldsymbol{v}(n) \tag{46}$$

where $\boldsymbol{C}_{m,q}$ is now the matrix corresponding to the Vandermonde vector formed by the root $\rho_{m,q}$. The μth receiver is composed of a bank of Q filters, each characterized by vectors $\boldsymbol{g}_{\mu,q}$ built from the Lagrange polynomial having all its roots $\rho_{i,j}$, $i = 1,\cdots,M$, $q = 1,\cdots,Q$, except $\rho_{\mu,q}$. Therefore, the μth receiver provides Q outputs

$$y_{\mu,q} = \boldsymbol{g}_{\mu,q}^T \boldsymbol{x}_\mu(n) = A_\mu H_\mu(\rho_{\mu,q}) s_\mu(n) + \boldsymbol{g}_{\mu,q}^T \boldsymbol{v}_\mu(n) \tag{47}$$

which can be combined to yield an estimate of $s_\mu(n)$. To evaluate the potential benefits coming from such a "*root diversity*," we adopted the maximal ratio combining (MRC) strategy, assuming that an error-free estimate of the channel is available. Supposing BPSK modulation, the decided symbol is given by

$$\begin{aligned} \hat{s}_\mu(n) &= \text{sign}\left(\sum_{q=1}^{Q} H_\mu^*(\rho_{\mu,q}) y_{\mu,q} \right) \\ &= \text{sign}\left(s_\mu(n) A_\mu^2 \sum_{q=1}^{Q} |H_\mu(\rho_{\mu,q})|^2 + w_\mu(n) \right) \end{aligned} \tag{48}$$

where $w_\mu(n) := \Sigma_{q=1}^{Q} H_\mu^*(\rho_{\mu,q}) \boldsymbol{g}_{\mu,q}^T \boldsymbol{v}_\mu(n)$.

The performance of MRC applied to our setup can be evaluated in terms of bit error rate (BER) by extending the classical derivations for MRC (see, e.g., [16]) when the fading coefficients are expressed in terms of the channel transfer functions $H_\mu(\rho_{\mu,q})$.

Using the Rayleigh channel model described in Section VI-A and assuming that the roots $\rho_{\mu,q}$ have the same modulus $\forall \mu$, the exponetially distributed random variables $|H_\mu(\rho_{\mu,q})|^2$ have the same expected value (and thus variance). In general, the rv's $|H_\mu(\rho_{\mu,q})|^2$ corresponding to different values of q are correlated. However, if we choose the roots as $\rho_{\mu,q} = \rho_\mu \exp(j2\pi q \Delta f)$, with $q = 0,\cdots,Q-1$ and $\Delta f > B_c$, where B_c is the channels' coherence bandwidth, the random variables $|H_\mu(\rho_{\mu,q})|^2$ are approximately uncorrelated. With this approximation, the average BER after MRC is [16, pp. 780–784]

$$P_e = \left(\frac{1-\beta}{2}\right)^Q \sum_{q=0}^{Q-1} \binom{Q-1+q}{q} \left(\frac{1+\beta}{2}\right)^q \tag{49}$$

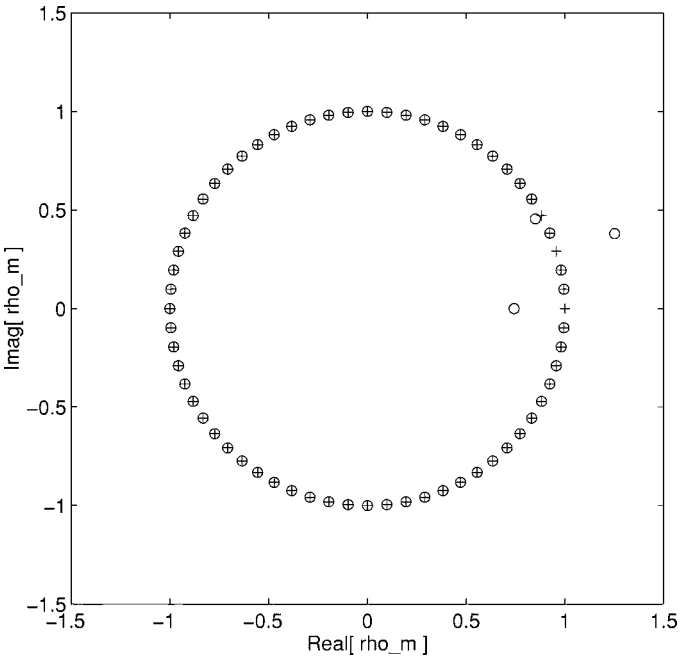

Fig. 10. Roots of the users: original location (+) and location after (o) root-control.

where $\beta := \sqrt{\gamma/(1+\gamma)}$, γ is the average SNR per channel, i.e., $\gamma := E\{|H_\mu(\rho_{\mu,q})|^2\}\mathcal{K}_{||}^2/\sigma_w^2$, and σ_w^2 is the variance of $\boldsymbol{g}_{\mu,q}^T \boldsymbol{v}_\mu(n)$. With γ sufficiently large, say, above 10 dB, P_e can be approximated as

$$P_e \approx \left(\frac{1}{4\gamma}\right)^Q \binom{2Q-1}{Q}. \tag{50}$$

Expression (50) is useful when it comes to choosing Q as a reasonable compromise between robustness and efficiency loss. Larger values of Q lead to lower BER values, but at the same time, they reduce the efficiency (measured as the number of information bits per transmitted symbol) by exactly a factor Q.

C. Root Hopping

Motivated by frequency-hopping ideas, in this subsection, we develop a nonredundant method to cope with channel fading using signature root hopping. Equations (37) and (40) suggest that the location of each user's signature root should be as far as possible from the channel roots. If the channel's roots are unknown, a strategy to avoid deep fades is to switch roots from symbol to symbol. Recall that the channel roots are no more than L, whereas the possible signature roots are $M > L$; therefore, not all codes will experience fading and the performance of each user will be close to the average predicted performance. Moreover, if the hopping pattern is specific of the cell, intercell interference can be mitigated by permuting the roots. Users at the edges of adjacent cells will not experience consistent interference from each other, even if they reuse their codes. Note that differential demodulation can be performed only among symbols corresponding to the same signature root. This can be achieved by including an interleaving (deinterleaving) operation such that the symbols pertaining to the same root are differen-

tially encoded (decoded). In addition, the channel should not vary faster than our root hopping rate.

Performance under our proposed root-hopping strategy, in terms of SNR_m and $P_e(\rho_m)$, can be obtained by averaging over $m = 1, \cdots, M$, (37), and (40), respectively. However, the advantage of the proposed technique can be appreciated by evaluating how far the real performance would be from its average with and without root hoping. To provide a reliable transmission link, not only good average performance is desired, but the variations around these averages should be small. On this subject. the following example illuminates the advantage of root hopping.

Example 6—Root Hopping: If R hops are designed for the mth user over the roots $\rho_1, \cdots, \rho_R$, the probability of error will equal the performance of the mth user, which is given by $P_e(\rho_r, \boldsymbol{h}_m)$ in (40), averaged over all the hops

$$P_e(\rho_m^{(1)}, \cdots, \rho_m^{(R)}, \boldsymbol{h}_m) = \frac{1}{R} \sum_{r=1}^{R} P_e(\rho_m^{(r)}, \boldsymbol{h}_m). \tag{51}$$

Using (40) for the error probability expression under the same assumptions on the channel vectors $\boldsymbol{h}_m$, the average probability of error is

$$E\{P_e\} = \frac{1}{R} \sum_{r=1}^{R} \frac{1}{1 + \overline{SNR}_r} \tag{52}$$

and its mean square can be derived using the general formula for the characteristic function of a quadratic form of Gaussian random vectors [1], and this is

$$E\{P_e^2\} = \frac{1}{R^2} \sum_{r,k=1}^{R} \frac{1}{|\boldsymbol{I} + \boldsymbol{R}_{h_m}(\alpha_r \boldsymbol{\rho}_r \boldsymbol{\rho}_r^{\mathcal{H}} + \alpha_k \boldsymbol{\rho}_k \boldsymbol{\rho}_k^{\mathcal{H}})|} \tag{53}$$

where $\boldsymbol{R}_{h_m}$ is the covariance matrix of the channel vector $\boldsymbol{h}_m$.

Fig. 11 shows the standard deviation of the error probability obtained without hopping (dashed line) and with hopping over $R = M = 16$ roots (solid line). The results have been obtained by averaging over 60 independent sets of channels and using, again, the Lagrange codes corresponding to the roots in Fig. 4. The channel model is the same as in Example 2. As expected, the variance of (51) decreases sensibly for $R = 16$, which shows that root hopping improves the reliability of the transmission link.

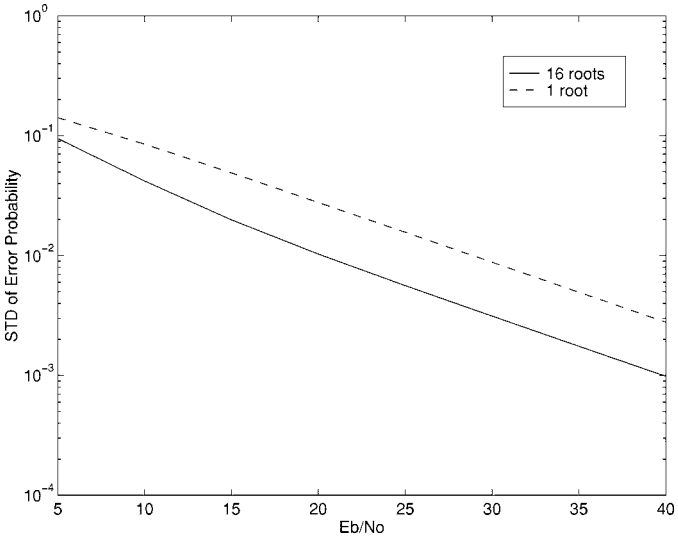

Fig. 11. Standard deviation of the error probability.

VIII. Concluding Remarks

We designed a general class of CDMA codes that guarantees channel-irrespective MUI elimination using simple linear receivers. The resulting LV-CDMA system generalizes the OFDMA scheme, but it provides several additional degrees of freedom, which can be exploited to add robustness against fading, carrier frequency offsets, and Doppler effects. Besides eliminating MUI, the proposed class of codes converts frequency-selective channels into flat fading channels. To combat the residual flat fading effects, we have introduced both nonredundant techniques, based on root hopping or root control, as well as redundant techniques based on maximum ratio combining. Furthermore, in view of the importance of long spreading codes used in IS-95 and the potential of accommodating users with variable rates, we developed the class of MUI-free long codes and LV-CDMA variable spreading codes. Our MUI-free variable rate coding scheme outperformed the Walsh-Hadamard-based scheme currently adopted for UMTS. Performance of the proposed LV/VL-CDMA transceivers was evaluated also analytically for transmissions over frequency-selective Rayleigh fading channels.

Because LV/VL designs require BS-user coordination or extra diversity to ameliorate flat fading effects, we currently investigate MUI– and fading-free transceiver designs. Preliminary results relying on symbol blocking and long codes are reported in [6].

Appendix

A. Proof of Proposition 1

Matrix (18) is a convolution matrix, and its left singular vectors are Vandermonde because $\forall \rho$

$$(1, \rho^{-1}, \cdots, \rho^{-P+1})\boldsymbol{C}_m = C_m(\rho)(1, \rho^{-1}, \cdots, \rho^{-L}) \tag{54}$$

where $C_m(z) := \Sigma_{k=0}^{M-1} c_m(k) z^{-k}$ is the $(M-1)$st order polynomial corresponding to the matrix $\boldsymbol{C}_m$. Clearly, from (54), the left null space of $\boldsymbol{C}_m$ is spanned by the Vandermonde vectors built from the roots of $C_m(z)$. When $C_m(z)$ has multiple roots, a basis for the null space of $\boldsymbol{C}_m$ should be built from the generalized Vandermonde (G-Vandermonde) vectors (see, e.g., [12]). The definition of the G-Vandermonde vectors is based on the property that if (and only if) ρ_0 is root of $C_m(\rho_0)$ with multiplicity $\geq k$, then for $i = 1, \cdots, k$

$$C_m(\rho_0) = \sum_{n=0}^{M-1} c_m(n)\rho_0^{-n} = 0 \Rightarrow \frac{d^{(i-1)}C_m(\rho_0)}{d(\rho^{-1})^{i-1}} = \sum_{n=i-1}^{M-1} c_m(n) \binom{n}{i} (\rho_0^{-1})^{n-i+1} = 0. \tag{55}$$

For every kth-order root ρ_0 of $C_m(\rho_0)$, we can define k independent G-Vandermonde vectors of length P as

$$\boldsymbol{\rho}_0^{(i)} = (\beta_i^0, \beta_i^1 \rho_0^{-1}, \cdots, \beta_i^{P-1} \rho_0^{-P+1}) \quad \text{where}$$
$$\beta_i^n := \begin{cases} \binom{n}{i}, & n \geq i \\ 0, & n < i. \end{cases} \tag{56}$$

Vector $\boldsymbol{\rho}_0^{(i)}$ is such that $\boldsymbol{\rho}_0^{(i)} \boldsymbol{C}_m = \mathbf{0}$ for $i \leq k$. When ρ_0 is not a root of $C_m(z)$ or a root with multiplicity less than i, the $L \times 1$ vector $\boldsymbol{\rho}_0^{(i)} \boldsymbol{C}_m \neq \mathbf{0}$ is not a G-Vandermonde anymore but a cumbersome function of the code polynomial derivatives (see, e.g., [12]). However, it is linearly independent from $\boldsymbol{\rho}_0^{(j)} \boldsymbol{C}_m$ with $j \neq i$.

From (18), since $\boldsymbol{C}_m$ in (18) has full column rank, the dimension of its null space is $P - (L+1) = M - 1$. Consider now an arbitrary vector $\boldsymbol{g}_\mu$ that satisfies (20). Since $\boldsymbol{g}_\mu$ belongs to all left null spaces of $\boldsymbol{C}_m$, $\forall m \neq \mu$, it can be expressed as

$$\boldsymbol{g}_\mu^{\mathcal{H}} = \sum_{k=1}^{M-1} \alpha_{\mu,m}(k) \boldsymbol{\rho}_{m,k}^{\mathcal{H}}, \quad \forall m \neq \mu \tag{57}$$

where $\boldsymbol{\rho}_{m,k}^{\mathcal{H}} := (1, \rho_{m,k}^{-1}, \cdots, \rho_{m,k}^{-P+1})$ is the Vandermonde vector built from the kth root $\rho_{m,k}$ of $C_m(z)$. In case of multiple roots, as many G-Vandermonde vectors as the root multiplicity will be introduced in the null-space basis of $\boldsymbol{C}_m$, but for simplicity, we will keep the notation $\rho_{m,k}$ unchanged. We will denote by $I_{\mu,m}$ the number of nonzero coefficients $\alpha_{\mu,m}(k)$ in the linear combination (57). The values $\rho_{m,k}$ with $k = 1, \cdots, M-1$ are assumed to be all distinct. Clearly, to avoid the undesired trivial null solution $\boldsymbol{g}_\mu = \mathbf{0}$, $I_{\mu,m}$ must be positive. To satisfy (20), the vector $\boldsymbol{g}_\mu$ in (57) must verify

$$\sum_{k=1}^{M-1} \alpha_{\mu,m}(k) \boldsymbol{\rho}_{m,k}^{\mathcal{H}} \boldsymbol{C}_i = \mathbf{0}^T, \quad \forall m \neq \mu, i \neq \mu. \tag{58}$$

On the other hand, according to (54), the product $\boldsymbol{\rho}_{m,k}^{\mathcal{H}} \boldsymbol{C}_i$ is still a Vandermonde vector, and Vandermonde vectors corresponding to distinct roots are linearly independent. If $\boldsymbol{\rho}_{m,k}$ is a G-Vandermonde corresponding to multiple roots, $\boldsymbol{\rho}_{m,k}^{\mathcal{H}} \boldsymbol{C}_i$ will also be linearly independent. Hence, (58) is valid if and only if $\forall i$, the $I_{\mu,m}$ roots $\rho_{m,k}$, corresponding to $\alpha_{\mu,m}(k) \neq 0$, are roots of $C_i(z)$. Considering (58) for all $i \neq \mu$ and $m \neq \mu$, it turns out that the generic ith polynomial $C_i(z)$ must have as roots the union set

$$\mathcal{S}_i = \bigcup_{\substack{\mu=1 \\ \mu \neq i}}^{M} \bigcup_{\substack{m=1 \\ m \neq \mu}}^{M} \{\{\rho_{m,k}\}_{k=1}^{M-1} \colon \alpha_{\mu,m}(k) \neq 0\} \tag{59}$$

where multiple roots are counted as many times as their multiplicity. When computing the cardinality of this set, we must recall that i) $I_{\mu,m} > 0$ and that ii) the number of roots of $C_i(z)$ is $M-1$, $\forall i$ (hence, the cardinality of $\mathcal{S}_i$ should be $M-1$). These two observations imply that the roots $\rho_{m,k}$ cannot be all different. Indeed, if they were all different, even if only one $\alpha_{\mu,m}(k) \neq 0$ for each (μ, m) pair, we would end up with a number of roots equal to $(M-1)^2$, which contradicts ii). Considering that (57) must be valid $\forall m \neq \mu$, the only possibility for the cardinality of $\mathcal{S}_i$ to be $M-1$ is that $I_{\mu,m} = 1, \forall m$. This proves that the vectors $\boldsymbol{g}_\mu$ are pure Vandermonde vectors or pure G-Vandermonde. Let us indicate the only nonzero term in (57) as $\boldsymbol{\rho}_\mu$. For every μ, this vector must be the same $\forall m \neq \mu$; hence, the corresponding ρ_μ must be a common root of $\boldsymbol{C}_m$, $\forall m \neq \mu$. Moreover, to guarantee that $\boldsymbol{g}_\mu^{\mathcal{H}} \boldsymbol{C}_\mu \neq \mathbf{0}^T$, $\forall \mu$, ρ_μ must not be a root of $C_\mu(z)$, and thus, the only possible choice for the roots is to select M distinct points ρ_m and assign $M-1$ of them to each polynomial, leaving out a different signature root for each user. Arguing by contradiction, this implies that the roots should have multiplicity one. Indeed, if in a certain code polynomial, say, $C_i(z)$, ρ_μ, has multiplicity greater than one, the degree of $C_i(z)$ would be $\geq M$ because $C_i(z)$ must also have all the other $M-2$ roots different from ρ_μ and from the signature root ρ_i. However, a code polynomial degree greater than $M-1$ is in contradiction with ii). This leads directly to our code design algorithm. ■

B. Proof of Proposition 2

From the definition of $C_m(z)$ in (21) and by setting $c_m(n) = \exp(j2\pi nm/M)$, we have

$$C_m(z) = \sum_{n=0}^{M-1} e^{j(2\pi/M)mn} z^{-n} = \frac{1 - z^{-M}}{1 - e^{j(2\pi/M)m} z^{-1}}. \tag{60}$$

Therefore, the $M-1$ roots of $C_m(z)$ are located on the unit circle at angles $2\pi\mu/M, \mu \in [0, M-1], \mu \neq m$. Because $C_m(z)$ is of order $M-1$, it follows that $c_m(n) = \exp(j2\pi nm/M)$ is the Lagrange polynomial (21) that interpolates the points $\rho_\mu = \exp(-j2\pi\mu/M)$, $\mu \neq m$ and $\mu = 0, \cdots, M-1$. ■

C. Proof of Proposition 3

Relying on the commutativity of convolution, we can interchange the $P \times (L+1)$ Toeplitz matrix $\boldsymbol{C}_m$ in (18) with the $1 \times P$ Vandermonde vector $\boldsymbol{g}_m^T = \boldsymbol{\rho}_m^T := (1, \rho_m^{-1}, \cdots, \rho_m^{-P+1})$.

If $\{\ell_m(n)\}_{n=0}^{P-1}$ are the mth Lagrange polynomial coefficients equal to $c_m(n)$ in the LV case, we obtain the product of the $P \times 1$ vector $(\ell_m(M-1), \cdots, \ell_m(0))^T$ with the $M \times (L+1)$ Toeplitz convolution matrix $\boldsymbol{V}_m$ built from the reversed Vandermonde vector $(\rho_m^{-P+1}, \cdots, 1)$:

$$\boldsymbol{V}_m = \begin{pmatrix} \rho_m^{-P+L+1} & \cdots & \rho_m^{-P+1} \\ \vdots & \ddots & \vdots \\ \vdots & \ddots & \vdots \\ 1 & \ddots & \rho_m^{-L}. \end{pmatrix} \tag{61}$$

Note that $\boldsymbol{V}_m = (\rho_m^{-M+1}, \cdots, 1)^T (1, \cdots, \rho_m^{-L})$ is a rank one matrix containing in its null space all vectors formed by the coefficients of the $(M-1)$st-order polynomials having ρ_m as a root; in particular, the Lagrange polynomials form a basis of its null space. Leading zeros select the last M rows of $\boldsymbol{C}_\mu(0)$, which, using the Vandermonde spreading codes, form

an $M \times (L+1)$ submatrix equal to $\boldsymbol{V}_m$ in (61). Inserting these expressions in (19), it is straightforward to verify that $\boldsymbol{g}_\mu^T \boldsymbol{C}_m \boldsymbol{h}_m = G_\mu(\rho_m)H(\rho_m) = \delta(m-\mu)G_m(\rho_m)H(\rho_m)$, where $G_\mu(z)$ is the polynomial corresponding to $\boldsymbol{g}_\mu$, i.e., $G_\mu(z) = \sum_{l=0}^{M-1} g_\mu(l)z^{-l}$. Therefore, building $\boldsymbol{g}_\mu$ so that $G_\mu(z)$ are the Lagrange polynomials

$$G_\mu(z) = \mathcal{L}_\mu(z) \tag{62}$$

we can satisfy the same conditions as (22) and (23) and achieve MUI elimination, as in (24).

This shows that VL design allows MUI cancellation with minimum spreading $P = M + L$, with $N_c > M$ and, in particular, with $N_c = P = M + L$. The question that arises is whether this dual VL design is also unique with the choice of $N_c = P + L$. Because $\boldsymbol{\nu}(\boldsymbol{C}_m(0)) \leq M-1$ and $\boldsymbol{\nu}(\boldsymbol{C}_m(1)) \leq N_c - P - L = M - 1$, (16) will be satisfied for all users only if the $M-1$ vectors $\boldsymbol{g}_\mu \ \forall \mu \neq m$ lie in the intersection $\mathcal{N}(\boldsymbol{C}_m(0)) \cap \mathcal{N}(\boldsymbol{C}_m(1))$. However, the structure of $\boldsymbol{C}_m(1)$ for $N_c = P = M + L$ characterizes completely its null space, independent of the code. Indeed, from (9), we observe that if $N_c = P = M + L$, the only nonzero elements of $\boldsymbol{C}_m(1)$ are contained in its first L rows that form an $L \times L$ full-rank upper-triangular submatrix. Therefore, $\mathcal{N}(\boldsymbol{C}_m(1))$ is spanned by the canonical vectors that select the last $M-1$ null rows of $\boldsymbol{C}_m(1)$, or in other words, the *only* possibility for having $\boldsymbol{g}_\mu^T \boldsymbol{C}_m(1) = \boldsymbol{0}^T$ is that $\boldsymbol{g}_\mu$ has L leading zeros. This is also why the only case of interest is $\boldsymbol{g}_m(k) = \boldsymbol{g}_m \delta(k)$. Due to the structure of $\mathcal{N}(\boldsymbol{C}_m(1))$, any $\boldsymbol{g}_m(k)$ should have leading zeros, with the nonzero part of $\boldsymbol{g}_m(k)$ determined only by $\boldsymbol{C}_m(0)$. Leading zeros determine the absence of residual ISI and render a higher order receiver unnecessary.

Having established the necessity of leading zeros, uniqueness of the VL design for $N_c = M + L$ and, thus, minimum spreading, comes from Proposition 1 as a byproduct of the commutativity of convolution. Indeed, if $\boldsymbol{g}_m$ is equipped with leading zeros, we are allowed to interchange the roles of $\boldsymbol{g}_m$ and the code vector $\boldsymbol{c}_m$ that defines the Toeplitz matrix $\boldsymbol{C}_m$. We thus arrive at a problem already addressed by Proposition 1 with a Sylvester matrix as in (18) that leads uniquely to the LV (here VL) design. ■

REFERENCES

[1] S. Betti, G. De Marchis, and E. Iannone, *Coherent Optical Communications Systems*. New York: Wiley, 1995, vol. B.

[2] S. Benedetto, E. Biglieri, and V. Castellani, *Digital Transmission Theory*. Englewood Cliffs, NJ: Prentice-Hall, 1987.

[3] S. E. Bensley and B. Aazhang, "Subspace-based channel estimation for code division multiple access communication systems," *IEEE Trans. Commun.*, vol. 44, pp. 1009–1020, Aug. 1996.

[4] L. J. Cimini, "Analysis and simulation of a digital mobile channel using orthogonal frequency division multiple access," *IEEE Trans. Commun.*, vol. COMM-33, pp. 665–675, 1985.

[5] K. Fazel and G. P. Fettweis, *Multi-Carrier Spread Spectrum*. Boston, MA: Kluwer, 1997.

[6] G. B. Giannakis, Z. Wang, A. Scaglione, and S. Barbarossa, "Mutually orthogonal transceivers for blind uplink CDMA irrespective of multipath channel nulls," in *Proc. Int. Conf. Acoust., Speech, Signal Process.*, vol. V, Phoenix, AZ, Mar. 15–19, 1999, pp. 2741–2744.

[7] F. van Heeyswyck, D. D. Falconer, and A. U. H. Sheikh, "A delay independent decorreoating detector for quasisynchronous CDMA," *IEEE J. Select. Areas Commun.*, vol. 14, pp. 1619–1626, Oct. 1996.

[8] ——, "Code selection for decorrelating detected quasisynchronous CDMA," in *Proc. 6th Int. Conf. Wireless Commun.*, vol. 2, July 1994, pp. 555–569.

[9] M. L. Honig, U. Madhow, and S. Verdú, "Blind adaptive multiuser detection," *IEEE Trans. Inform. Theory*, vol. 41, pp. 944–996, 1995.

[10] R. A. Iltis, "Demodulation and code acquisition using decorrelator detectors for quasisynchronous CDMA," *IEEE Trans. Commun.*, vol. 44, pp. 1553–1560, 1996.

[11] H. Liu and G. Xu, "A subspace method for signature waveform estimation in synchronous CDMA systems," *IEEE Trans. Commun.*, vol. 44, pp. 1346–1354, 1996.

[12] L. Lupas, "On the computation of generalized Vandermonde matrix inverse," *IEEE Trans. Automat. Contr.*, vol. AC-20, pp. 559–561, 1975.

[13] R. Lupas and S. Verdú, "Near-far resistance of multiuser detectors in asynchronous channels," *IEEE Trans. Commun.*, vol. 38, pp. 496–508, 1990.

[14] U. Madhow, "MMSE Interference suppression for direct-sequence spread-spectrum CDMA," *IEEE Trans. Commun.*, vol. 44, pp. 3178–3188, 1994.

[15] E. Nikula, A. Toskala, E. Dahlman, L. Girard, and A. Klein, "FRAMES multiple access for UMTS and IMT-2000," *IEEE Personal Commun.*, vol. 41, pp. 16–24, Apr 1998.

[16] J. G. Proakis, *Digital Communications*, 2nd ed. New York: McGraw-Hill, 1989, pp. 722–725.

[17] A. Scaglione and G. B. Giannakis, "Design of user codes in QS-CDMA systems for MUI elimination in unknown multipath," *IEEE Commun. Lett.*, vol. 3, pp. 25–27, Feb. 1999.

[18] V. M. Da Silva and E. S. Sousa, "Multicarrier orthogonal CDMA signals for quasisynchronous communication systems," *IEEE J. Select. Areas Commun.*, vol. 12, pp. 842–852, 1994.

[19] N. Suehiro, "A signal design without co-channel interference for approximately synchronized CDMA systems," *IEEE J. Select. Areas Commun.*, vol. 12, pp. 837–841, June 1994.

[20] M. K. Tsatsanis, "Inverse filtering criteria for CDMA systems," *IEEE Trans. Signal Processing*, vol. 45, pp. 102–112, Jan. 1997.

[21] M. K. Tsatsanis and G. B. Giannakis, "Multirate filter banks for code-division multiple access systems," in *Proc. Int. Conf. ASSP*, vol. 2, New York, 1995, pp. 1484–1487.

[22] ——, "Optimal linear receivers for DS-CDMA systems: A signal processing approach," *IEEE Trans. Signal Processing*, vol. 44, pp. 3044–3055, Nov. 1996.

[23] M. K. Tsatsanis and Z. Xu, "Performance analysis of minimum variance CDMA receivers," *IEEE Trans. Signal Processing*, vol. 46, pp. 3014–3022, Nov. 1998.

[24] S. Verdú, *Multiuser Detection*. Cambride, U.K.: Cambridge Univ. Press, 1998.

[25] X. Wang and V. Poor, "Blind equalization and multiuser detection in dispersive CDMA channels," *IEEE Trans. Commun.*, vol. 46, pp. 91–103, Jan. 1998.

Anna Scaglione (M'99) received the M.Sc. and Ph.D. degrees in electrical engineering from the University of Rome "La Sapienza," Rome, Italy, in 1995 and 1999, respectively.

During 1997, she visited the University of Virginia (UVA), Charlottesville, as a Research Assistant. She is currently a Post Doctoral researcher at the University of Minnesota, Minneapolis. Her research interests are in statistical signal processing and communication theory.

Georgios B. Giannakis (F'96) received the Diploma in electrical engineering from the National Technical University of Athens, Athens, Greece in 1981. From September 1982 to July 1986, he was with the University of Southern California (USC), Los Angeles, where he received the M.Sc. degree in electrical engineering in 1983, the M.Sc. degree in mathematics in 1986, and the Ph.D. degree in electrical engineering in 1986.

After lecturing for one year at USC, he joined the University of Virginia (UVA), Charlottesville, in 1987, where he became a Professor of electrical engineering in 1997, Graduate Committee Chair, and Director of the Communications, Controls, and Signal Processing Laboratory in 1998. Since January 1999, he has been with the University of Minnesota, Minneapolis, as a Professor of electrical and computer engineering. His general interests lie in the areas of signal processing and communications, estimation and detection theory, time-series analysis, and system identification—subjects on which he published more than 100 journal papers. Specific areas of expertise have included (poly)spectral analysis, wavelets, cyclostationary, and non-Gaussian signal processing with applications to sensor array and image processing. Current research focuses on transmitter and receiver diversity techniques for equalization of single- and multiuser communication channels, mitigation of rapidly fading channels, compensation of nonlinear amplifier effects, redundant filterbank transceivers for block transmissions, multicarrier, and wideband communication systems.

Dr. Giannakis was awarded the School of Engineering and Applied Science Junior Faculty Research Award from UVA in 1988 and the UVA-EE Outstanding Faculty Teaching Award in 1992. He received the IEEE Signal Processing Society's 1992 Paper Award in the Statistical Signal and Array Processing (SSAP) area and the 1999 Young Author Best Paper Award (with M. K. Tsatsanis). He co-organized the 1993 IEEE Signal Processing Workshop on Higher-Order Statistics, the 1996 IEEE Workshop on Statistical Signal and Array Processing, and the first IEEE Signal Processing Workshop on Wireless Communications in 1997. He guest (co-)edited two special issues on high-order statistics (*International Journal of Adaptive Control and Signal Processing* and the EURASIP journal *Signal Processing*) and the January 1997 Special Issue on Signal Processing for Advanced Communications of the IEEE TRANSACTIONS ON SIGNAL PROCESSING. He has served as an Associate Editor for the IEEE TRANSACTIONS ON SIGNAL PROCESSING and the IEEE SIGNAL PROCESSING LETTERS, a Secretary of the Signal Processing Conference Board, a member of the SP Publications Board, and a member and vice-chair of SSAP Technical Committee. He now chairs the Signal Processing for Communications Technical Committee and serves as Editor-in-Chief of the IEEE SIGNAL PROCESSING LETTERS. He is also a member of the IEEE Fellow Election Committee, the IMS, and the European Association for Signal Processing.

Sergio Barbarossa (M'88) received the M.Sc. and Ph.D. degrees in electrical engineering from the University of Rome "La Sapienza," Rome, Italy, in 1984 and 1988, respectively.

From 1984 to 1986, he was a Radar System Engineer with Selenia, Rome, Italy. Since 1986, he has been with the Information and Communication Department, University of Rome "La Sapienza," where he is an Associate Professor. In 1988, on leave from the University of Rome, he was a Research Engineer with the Environmental Research Institute of Michigan, Ann Arbor. During the spring of 1995 and the summer of 1997, he was a visiting faculty member with the Department of Electrical Engineering, University of Virginia, Charlottesville, and from March 1999 to August 1999, he was a Visiting Professor with the University of Minnesota, Minneapolis. He has been involved in several international projects concerning phased array radars, synthetic aperture radars, and mobile communication systems. His current research activity is in the area of broadband mobile communication systems with specific attention to multiple access systems, optimal coding, synchronization, channel estimation, tracking, and equalization.

Dr. Barbarossa is a member of the IEEE Technical Committee on Signal Processing for Communications and is currently serving as an Associate Editor for the IEEE TRANSACTIONS ON SIGNAL PROCESSING.